DETERMINATION OF THE g-FACTOR FOR SEVERAL SHORT-LIVED NUCLEAR STATES

Thesis by

John D. Rogers

In Partial Fulfillment of the Requirements

For the Degree of

Doctor of Philosophy

California Institute of Technology

Pasadena, California

1961

ACKNOWLEDGMENTS

The experiments reported in this thesis were conceived by Dr. Geoffrey Manning. I am most grateful for the opportunity of collaborating with him on their realization. Many of the results reported here are the fruits of this collaboration; however, the studies in Tm^{169}, Dy^{160}, and Er^{166} were carried out by the author alone.

I would like to thank Professor Felix Boehm for his supervision and advice during the final stages of this research and the preparation of this thesis. I am indebted to Dr. Ulrich Hauser for valuable advice and encouragement. It is a further pleasure to acknowledge the assistance of Mr. Herbert Henrikson in the design and construction of equipment for this experiment.

The success of any experiment such as this depends to a great extent on the facilities and atmosphere of the laboratory in which they are done, and I must therefore express my appreciation to Professor J. W. M. DuMond for the opportunity of working under him during the past four years. I would also like to mention the pleasure and profit gained from my associations with the present and past members of the research group here.

This research was conducted under a contract with the United States Atomic Energy Commission.

ABSTRACT

The g-factors of nine excited nuclear states have been measured by observing the rotation of the angular correlation of a γ-γ cascade in a magnetic field whose direction was alternately switched up and down with respect to the plane of the measurement. The results are: 280-kev state of As^{75} ($\tau = 4 \times 10^{-10}$ sec) $g = (0.39 \pm 0.12)$; 91-kev state of Pm^{147} ($\tau = 3.4 \times 10^{-9}$ sec) $g = (0.93 \pm 0.20)/G_2$, where G_2 is between 0.5 and 1.0 ; 118-kev state of Tm^{169} ($\tau = 9.0 \times 10^{-11}$ sec) $g = (0.21 \pm 0.07)$; 114-kev state of Lu^{175} ($\tau = 9.4 \times 10^{-11}$ sec) $g = (0.65 \pm 0.25)$; 113-kev state of Hf^{177} ($\tau = 7 \times 10^{-10}$ sec) $g = (0.20 \pm 0.06)$; 122-kev state of Sm^{152} ($\tau = 2.0 \times 10^{-9}$ sec) $g = (0.28 \pm 0.07)$; 123-kev state of Gd^{154} ($\tau = 1.7 \times 10^{-9}$ sec) $g = (0.4 \pm 0.5)$; 87-kev state of Dy^{160} ($\tau = 2.6 \times 10^{-9}$ sec) $g = (0.28 \pm 0.08)$; 81-kev state of Er^{166} ($\tau = 2.4 \times 10^{-9}$ sec) $g = (0.31 \pm 0.06)$. The measurements have been compared to theoretical predictions. On the basis of the shell model, the probable value of the spin for the 91-kev level of Pm^{147} is 5/2+ . The results for Tm^{169}, Lu^{175}, and Hf^{177} have been interpreted using the Nilsson model. The results found are in qualitative agreement with theory, but some deviations, especially in Hf^{177}, are noted. The measurements for the 2+ states of Sm^{152}, Dy^{160}, and Er^{166} provide a direct evaluation of the rotational g-factor, g_R , of the collective model. The values found are about 3/4 of the value $g_R = Z/A$ predicted for uniform nuclear flow. The effects of electronic paramagnetism in rare earths on these measurements are treated in an appendix. The assumptions necessary to interpret the observed rotation in terms of the g-factor are discussed.

TABLE OF CONTENTS

LIST OF FIGURES

LIST OF TABLES

I. INTRODUCTION

The magnetic dipole moment, together with the nuclear spin, was one of the first properties of the atomic nucleus to be studied extensively, and its determination is still of considerable interest to the nuclear physicist. Techniques such as interpretation of optical hyperfine structure, atomic and molecular beams, and magnetic resonance, have furnished a wealth of data on the moments of nuclear ground states. Values of the magnetic moment for excited states of nuclei, contrastingly, are at present very sparse since, because of the short lifetimes of such states, the above mentioned techniques generally fail to apply.

In 1950, Brady and Deutsch[1] pointed out that the recently verified existence of anisotropic angular correlations in γ-ray cascades made possible a new method for measuring g-factors of some short-lived nuclear states. This technique, observation of the change in an angular correlation in a magnetic field applied perpendicular to the plane of the correlation measurement, was first used by Aeppli, Albers-Schonberg, Bishop, Frauenfelder, and Heer to determine the magnetic moment of the first excited state of Cd^{111} [2]. Generalizations of the technique have since been used by several workers to study various nuclear states[3] with lifetimes as short as 10^{-9} sec.

This thesis discusses the measurement of g-factors for nine excited nuclear states whose mean lifetime varied from 2.5×10^{-9} sec. to 9×10^{-11} sec. The advanced techniques developed for this experiment, though based on the principle suggested by Brady and Deutsch, made possible the measurement of extremely small changes through the minimization of systematic field effects and the effects of

instrumental fluctuations. This allowed the study of states whose lifetime was less than 10^{-10} sec. and whose rotation in the applied field during this time was, in the most favorable case, only 0.2 degrees.

The extension of the lifetime range below 10^{-9} sec. has made possible the study of many of the low-lying states in the region of large nuclear deformations, thus greatly expanding the scope of the technique. The properties of these states are at present of considerable interest to the collective and unified nuclear models.

The first sections of this thesis are devoted to a discussion of the results of the theory of angular correlations important to this experiment. The application of these results to the measurements is shown. A section is given to the description of the equipment and the experimental technique. The experimental results for each nuclear state, and comparison to theoretical predictions are treated in the next two sections. A discussion of the experiment and its results concludes the thesis.

II. PRINCIPLES OF ANGULAR CORRELATIONS

2.0 Introduction

For the interpretation of the experimentally observed change in the angular correlation of a γ-ray cascade when an external magnetic field is applied, certain of the concepts and formulas from the theory of angular correlations are required. In the following sections a brief review of this theory is presented, first under the assumption that interactions of the nucleus during the intermediate state are negligible, and then considering the interactions with internal fields. Following this, the effects of a static magnetic field on such angular correlations are discussed, and the application of the effect to the measurement of nuclear g-factors is shown. Most of the results discussed here are more completely developed in the articles of Devons and Goldfarb[4], and of Abragam and Pound[5].

2.1 Unperturbed Angular Correlations

The particular case of interst is that of a γ-ray cascade, as illustrated in Fig. 1, in which a level of spin I_i and energy E_o decays by emission of γ-ray γ_1 of mixed multipolarity L_1, L_1' to a state of energy E_1, spin I, and mean lifetime τ. This state emits γ_2 of mixed multipolarity L_2, L_2' going to the final state of spin I_f and energy E_f.

In general, if one measures the coincidence counting rate for γ_1 and γ_2 detected in counters D_1 and D_2, respectively, in a geometry as illustrated in Fig. 2, then as a function of the angle θ

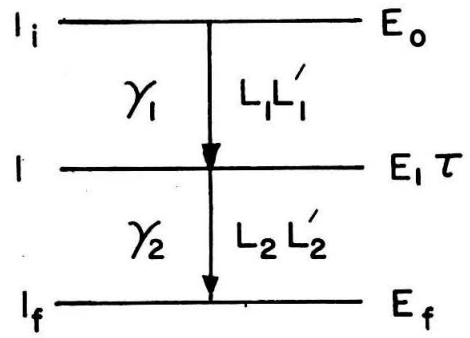

Figure 1. Typical Level Scheme. The Terms Are Defined in the Text.

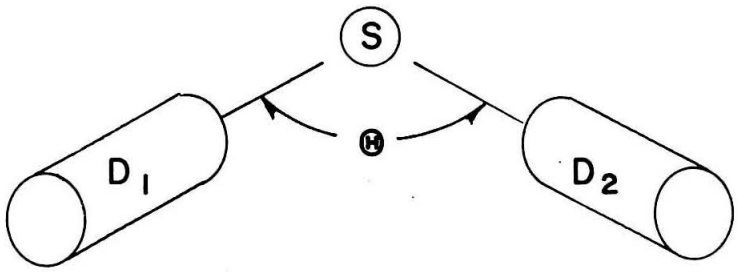

Figure 2. Typical Counting Geometry. The Symbols Are Defined in the Text.

between the γ-rays, the normalized counting rate, $W(\theta)$ can be expressed as

$$W(\theta) = \sum_{\text{even } k} A_k P_k(\cos\theta), \qquad (1)$$

with $A_o = 1$ ($P_k(\cos\theta)$ are the Legendre polynomials of order k). In the cases of interest to this work, all correlations are of the form

$$W(\theta) = 1 + A_2 P_2 (\cos \theta) + A_4 P_4 (\cos \theta) \qquad (2)$$

If the geometry of the experiment is such that corrections for the finite solid angle subtended by the counters are negligible, and if the source strength is low enough that the random coincidence counting rate is insignificant, then the A_k's in Eq. (1) depend only on the spins I_i, I, I_f, and the multipolarities L_1, L_1' and L_2, L_2' of γ_1 and γ_2 respectively, provided that the nucleus does not interact significantly with any internal or external field during the lifetime of the intermediate state.

2.2 Perturbed Angular Correlations

Effects ascribable to the interaction of the nucleus with internal fields of the source have been observed in many angular correlation experiments. Both the interaction of the nuclear electric quadripole moment with the gradient of the local electric field, and the coupling of the magnetic dipole moment with the internal magnetic fields can be significant.

Qualitatively, the effects of such interactions can be understood in the following way. For the theoretical values of the A_k's in Eq. (1) to be realized, it is necessary that the nuclear alignment remain unchanged for the duration of the intermediate state. The internal fields, however, cause precessions of the nucleus which change the alignment and thereby affect the correlation coefficients.

To clarify such effects, we may consider the example of an atomic nucleus interacting with the fluctuating electric field gradients in a liquid. These field gradients change rapidly in both direction

and amplitude due to the thermal motion of the atom. It is convenient to define the average time the field gradient at the nucleus stays constant in direction as τ_c. This time is closely related to the time between collisions and is estimated in Ref. 5 to be somewhat less than 10^{-11} sec. for a typical ion in water. The electric field gradient exerts a torque on the nuclear quadripole moment which causes it to precess around the direction of the field gradient with an approximate angular frequency

$$\omega_i = \frac{eQ}{\hbar}\left(\overline{\frac{\partial E}{\partial z}}\right),$$

where $\overline{(\partial E/\partial z)}$ is the average electric field gradient, and Q is the nuclear electric quadripole moment. During the time τ_c, the nucleus will precess through an angle $\omega_i \tau_c$ around the field gradient. If τ_c is much shorter than the nuclear lifetime, τ, then the nuclear spin axis will undergo a series of small precessions around arbitrary space axes during the intermediate state. The result will be a "smearing" of the nuclear alignment and a consequent attenuation of the angular correlation.

The amount of "smearing" of the nuclear alignment is dependent on the time between γ_1 and γ_2 (see Fig. 1). Abragam and Pound[5] show that the effect of the fluctuating fields on the angular correlation of Eq. (1) is such that the correlation when the time between the two γ-rays is exactly t can be written as

$$W(\theta) = \sum_k A_k G_k(t) P_k(\cos\theta)$$

$$\text{with } G_k(t) = e^{-\lambda_k t} \qquad (3)$$

They give explicit formulas for the inverse times $1/\lambda_k$. The λ_k's are proportional to $\omega_i^2 \tau_c$ and λ_1 is the inverse of the spin lattice relaxation time measured by resonance techniques.

Since the probability of a nucleus emitting γ_2 at time t is proportional to $e^{-t/\tau}$, the resulting angular correlation measured with a coincidence system whose resolving time $2\tau_R \gg \tau$ can be written as

$$W(\theta) = \frac{1}{\tau} \int_0^\infty \sum_k A_k P_k(\cos\theta)\, e^{-\lambda_k t}\, e^{-t/\tau}\, dt . \qquad (4)$$

When this is integrated, one finds

$$W(\theta) = \sum_k A_k G_k P_k(\cos\theta)$$
$$\text{with } G_k = 1/(1 + \lambda_k \tau) \quad . \qquad (5)$$

For a typical nucleus in a liquid, $\tau_c \sim 10^{-12}$ sec. and $\omega_i = 10^{10}$ radians per sec. are reasonable figures. Thus, the approximations $\omega_i \tau_c \ll 1$ and $\tau_c \ll \tau$ are valid (no attenuation can be expected from this effect for $\tau < 10^{-11}$ sec.). Accurate estimates of τ_c and the average field gradients $\overline{(\partial E/\partial z)}$ are not available in most cases, and therefore, only order of magnitude estimates of the G_k's are possible. For a nucleus with a quadripole moment of 1 barn, significant effects can be seen when $\tau = 10^{-8}$ sec.

Internal magnetic fields strong enough to cause attenuation of angular correlations can result from electronic paramagnetism of the atom containing the nucleus. The paramagnetic rare earth ions,

for instance, generate fields of several million gauss at their nuclei. These strong magnetic fields have the same fluctuating character as the electric fields discussed above for rare earth ions in solution, since the electronic angular momentum is constantly changing in direction from collisions.

If τ_c is now redefined as the time the magnetic field stays constant in direction, the estimate $\tau_c \sim 10^{-12}$ sec. is again reasonable. If the field strength is H, the nuclei will precess around the magnetic field with the Larmor frequency,

$$\omega_L = - g \frac{\mu_n}{\hbar} H , \qquad (6)$$

where g is the nuclear g-factor, and μ_n the nuclear magneton. With $H = 10^6$ gauss and $g = 1$, this precession frequency is again 10^{10} radians per sec. The assumptions $\omega_L \tau_c << 1$ and $\tau_c << \tau$ hold for the cascades of interest in most rare earth ions, and the analysis leading to Eqs. (3), (4) and (5) is still valid when the parameters λ_k are redefined (see Ref. 5). The λ_k's are now proportional to $\omega_L^2 \tau_c$, and using the formulas of Ref. 5 with $\tau_c = 10^{-12}$ sec., significant attenuation is found for $g = 1$, $\omega_L = 10^{10}$ radians per sec., when τ is longer than 2×10^{-9} sec. Again, appropriate values of τ_c are only approximately known, so that this estimate can only be an order of magnitude one.

Although all of the experiments reported here were done in liquid sources, a short comment can be made about the attenuation effects in solids. As mentioned in Ref. 5, the significant electric fields in solids are static fields. Therefore, even for small rotational frequencies the angle smearing effect may be quite large

(the rotation angle is $\omega_i \tau$ instead of $\omega_i \tau_c$). The average electric field gradient will depend upon whether the atom is moved from its lattice position by the recoil of the first γ-ray (or a previous nuclear disintegration). Attenuation in solid sources is typically much greater than in liquids for the same cascade. Magnetic fields in rare earth paramagnetic solids, conversely, fluctuate very rapidly, typical values of τ_c being 10^{-12} to 10^{-13} sec. The effects of such fields can be expected to be similar in solids and liquids.

2.3 Angular Correlations in Applied Magnetic Fields

The effects of applied external magnetic fields on such angular correlations are easily seen. To illustrate the result, one can first consider the case where the perturbing fields in the intermediate state are negligible. If a magnetic field H_{eff} is applied along the z axis perpendicular to the plane of the angular correlation measurement, the nuclear spin axis will precess around the field with a frequency

$$\omega = \frac{-g \mu_n H_{eff}}{\hbar} \tag{7}$$

If all the nuclei lived a time τ between the emission of γ_1 and γ_2, then the angular correlation of Eq. (1) would become

$$W(\theta) = \sum A_k P_k(\cos(\theta + \omega\tau)) \tag{8}$$

In the more general case, where the nuclear state decays exponentially, the time integrated correlation (for $2\tau_R >> \tau$) becomes

$$W(\theta, H) = \frac{1}{\tau} \int_0^\infty \sum_k A_k P_k \left(\cos(\theta + \omega t)\right) \; e^{-t/\tau} \, dt \quad . \tag{9}$$

Calculation of this integral is simplified by writing the correlation of Eq. (1) in the equivalent form

$$W(\theta) = \sum_k C_k \cos(k\theta) \, ,$$

$$\text{with } C_o = 1 \, . \tag{10}$$

Equation (9) then becomes

$$W(\theta, H) = \frac{1}{\tau} \int_o^\infty \sum_k C_k \cos k(\theta + \omega t) \, e^{-t/\tau} \, dt \, , \tag{11}$$

which, when integrated, becomes

$$W(\theta, H) = \sum_k \frac{C_k}{\left[1 + (k\omega\tau)^2\right]^{\frac{1}{2}}} \cdot \cos k(\theta + \Delta\theta_k) \, ,$$

$$\text{with} \quad \Delta\theta_k = \frac{1}{k} \tan^{-1} k\omega\tau \quad . \tag{12}$$

The resulting angular correlation (undisturbed by internal fields) is both rotated and attenuated compared to that in zero field.

In the case of time dependent electric quadripole attenuation (as occurs in liquid sources), Eq. (9) must be rewritten to include $G_k(t)$. It becomes

$$W(\theta, H) = \frac{1}{\tau} \int_o^\infty \sum_k A_k P_k(\cos(\theta + \omega t)) e^{-t/\tau} \, e^{-\lambda_k t} \, dt \quad . \tag{13}$$

The value of this integral is not hard to obtain, but is difficult to write in closed form. For $k = 4$, it becomes

$$W(\theta, H) = 1 + \frac{G_2 A_2}{4}\left[1 + \frac{3\cos 2(\theta + \Delta\theta_{22})}{\left[1 + (2G_2\omega\tau)^2\right]^{\frac{1}{2}}}\right] +$$

$$\frac{G_4 A_4}{64}\left[9 + \frac{20\cos 2(\theta + \Delta\theta_{24})}{\left[1 + (2G_4\omega\tau)^2\right]^{\frac{1}{2}}} + \frac{35\cos 4(\theta + \Delta\theta_{44})}{\left[1 + (4G_4\omega\tau)^2\right]^{\frac{1}{2}}}\right] .$$

$$\Delta\theta_{22} = \tfrac{1}{2}\tan^{-1} 2G_2\omega\tau \quad , \qquad \Delta\theta_{24} = \tfrac{1}{2}\tan^{-1} 2G_4\omega\tau \quad ,$$

$$\Delta\theta_{44} = \tfrac{1}{4}\tan^{-1} 4G_4\omega\tau .$$

If G_k 1, i.e. the rotation is through a small angle, the result can be approximated for all k as

$$W(\theta, H) = \sum_k A_k G_k P_k (\cos(\theta + G_k\omega\tau)) . \qquad (15)$$

The terms in the angular correlation in zero field thus appear rotated through an angle $G_k\omega\tau$ when the external field is applied. This illustrates that the attenuation coefficients G_k must be known independently in order to measure $\omega\tau$ from the observed rotation.

When a static magnetic field is applied to a source in which attenuation due to hyperfine interaction exists, several different possibilities must be considered. If we define the Larmor precession frequency of the electronic angular momentum in the field H as

$$\omega_e = -g_e \frac{\mu_o}{h} H ,$$

where g_e is the electronic g factor and μ_o the Bohr magneton, then we may consider the two cases $\omega_e >> 1/\tau_c$ and $\omega_e << 1/\tau_c$ (τ_c is the time the magnetic field at the nucleus stays constant in direction). When $\omega_e << 1/\tau_c$, the electron cannot precess significantly around the external field before it undergoes a phase changing transition, and therefore the external magnetic field does not affect the electron-nucleus interaction. As a result, the derivation leading to Eqs. (14) and (15) still holds, and these formulas can be used in this case with the G_k's measured in zero field. In almost all rare earths, $\tau_c \sim 10^{-12}$ sec. and the approximations used in the above discussion are valid.

If $\omega_e \geq 1/\tau_c$ and as well $\omega_e >> \omega_L$ (the Larmor frequency of the nucleus in the electron field), the nucleus interacts with the average projection of the internal field on the axis of the applied field. In this case, the attenuation effects are dependent upon the direction of the applied field with respect to the directions the γ-rays are measured. Such a field applied along the direction of one of the γ-rays can completely remove hyperfine attenuation, while if it is applied perpendicular to the plane of the correlation measurement, the attenuation increases. τ_c is relatively long for the Gd^{3+} ion in the rare earths, and for most of the iron group paramagnetics, and therefore such effects may be observed with these ions.

When $\tau_c << \tau$ in a paramagnetic source, there is a further effect on angular correlations in applied magnetic fields to be considered. The external field in this case induces an average po-

larization of the electronic moment (giving rise, for instance, to paramagnetic susceptibility) and therefore the field at the nucleus is not the applied field, but can be written as

$$H_{eff} = \beta H \tag{16}$$

where H_{eff} and H are respectively the effective and the applied fields. The paramagnetic correction factor β for rare earth 3+ ions is calculated in Appendix I assuming $\tau_c << \tau$ and also that the electronic structure is in thermal equilibrium for the duration of the intermediate state in the configuration of the 3+ daughter ion. The validity of these assumptions is discussed in the appendix. The effect on the angular correlations discussed can be found by substituting Eq. (16) into Eq. (7) for the Larmor frequency, all other formulas remaining unchanged.

The two cases discussed above cover most situations of interest for angular correlation experiments using liquid sources. Abragam and Pound[5] give some discussion of the effects to be expected when solid sources are used. In a solid polycrystalline substance in which large static electric field gradients exist along with a large enough hyperfine interaction to cause attenuation of the angular correlation, the interpretation of angular correlation rotation results could be quite difficult. Because of the complexity of this problem, results obtained from experiments using solid sources must be considered somewhat carefully.

III. DESCRIPTION OF THE EXPERIMENT

3.0 Experimental Method

Each g-factor measurement consisted of two parts; first, a measurement of the angular correlation; and second, a measurement of the rotation due to the applied magnetic field.

The observed angular correlation, corrected for random coincidence and finite solid angle of the counters is compared to the theoretical prediction and those of other experimenters to determine (wherever possible) the attenuation coefficients G_k. A measurement of these parameters to better than 5% was never necessary for these experiments.

The rotation was measured by setting the counter at the point where $dW(\theta)/d\theta$ was a maximum and measuring the counting rate with field up and field down. From these counting rates, one can form the number

$$R = \frac{W(\theta, H) - W(\theta, -H)}{\frac{1}{2} W(\theta, H) + W(\theta, -H)} \quad . \tag{17}$$

Using Eq. (14) or Eq. (15) along with the observed value of the angular correlation (uncorrected for finite solid angle, random coincidences, or the presence of competing cascades through short half-life states) and the attenuation parameters, G_k, a value of $\omega\tau$ can be deduced from the observed value of R. From this value of $\omega\tau$, a value of g can be calculated. Recalling Eqs. (7) and (16),

$$H_{eff} = \beta H \qquad \text{and} \tag{16}$$

$$\omega = -g \frac{\mu_n}{\hbar} H_{eff} \quad , \tag{7}$$

one finds that

$$g = -\frac{\hbar}{\mu_n} \frac{\omega}{\beta H} \quad . \tag{18}$$

For the case where the observed correlation is describable as

$$W(\theta) = 1 + C_2 \cos 2\theta \, , \tag{19}$$

the optimum angles are $\pi/4$, $3\pi/4$, $5\pi/4$ or $7\pi/4$, and when Eq. (15) applies, we can write

$$R = \frac{W(\theta, H) - W(\theta, -H)}{\frac{1}{2}[W(\theta, H) + W(\theta, -H)]} = \mp 4 C_2 \omega \tau G_2 \, ,$$

$$G_2 \omega \tau = \mp \frac{R}{4 C_2} \, , \tag{20}$$

$$g = \pm \frac{\hbar}{\mu_n} \frac{R}{4 C_2 G_2 \tau H_{eff}} \, ,$$

where the upper sign applies for $\theta = \pi/4$ or $5\pi/4$ and the lower for $\theta = 3\pi/4$ or $7\pi/4$.

Two different checks were made on the results in certain cases. If the angle between the counters is changed from θ to $(2\pi - \theta)$, the value of R should change sign. This may be accomplished without moving the counters by adjusting the electronic settings so that the γ-rays accepted by the counters are interchanged. Any systematic field effects will not be reversed, and their presence can be detected.

The second check is available when one of the γ-rays has a significant K-conversion coefficient. These γ-rays together with the K x-rays which are in coincidence with the other γ-rays of the cascade are recorded in the pulse height analyzer. The angular correlation of the K x-rays is isotropic, and hence R for the γ-ray – x-ray cascade should be zero. This value thus provides a check on systematic effects.

In the cases where such x-rays have been observed, the angular correlation was usually measured by normalizing the counting rate at each angle to the x-ray. The value for R in these cases is also quoted with an error which includes both the γ-ray counting statistics and the K x-ray counting statistics. In Er^{166}, this procedure was not followed, because the effect was so large that the possible systematic effects were completely negligible.

As an illustration of a typical measurement, Fig. 3 shows the angular correlation observed for the 208-113 kev cascade in Hf^{177} (see Section 4.5). The two broken curves are the correlation for field up and field down respectively. The circles show the observed counting rates at 135° and 225° for the two directions of the field. The observed rotation was (0.0091 ± 0.0014) radians, or (0.52 ± 0.08) degrees. The intermediate state lifetime is $\tau = 7 \times 10^{-10}$ sec., and the calculated g-factor, $g = 0.20 \pm 0.06$.

3.1 Equipment and Experimental Details

A g-factor determination consisted of two parts; measurement of the angular correlation for the cascade of interest, and measure-

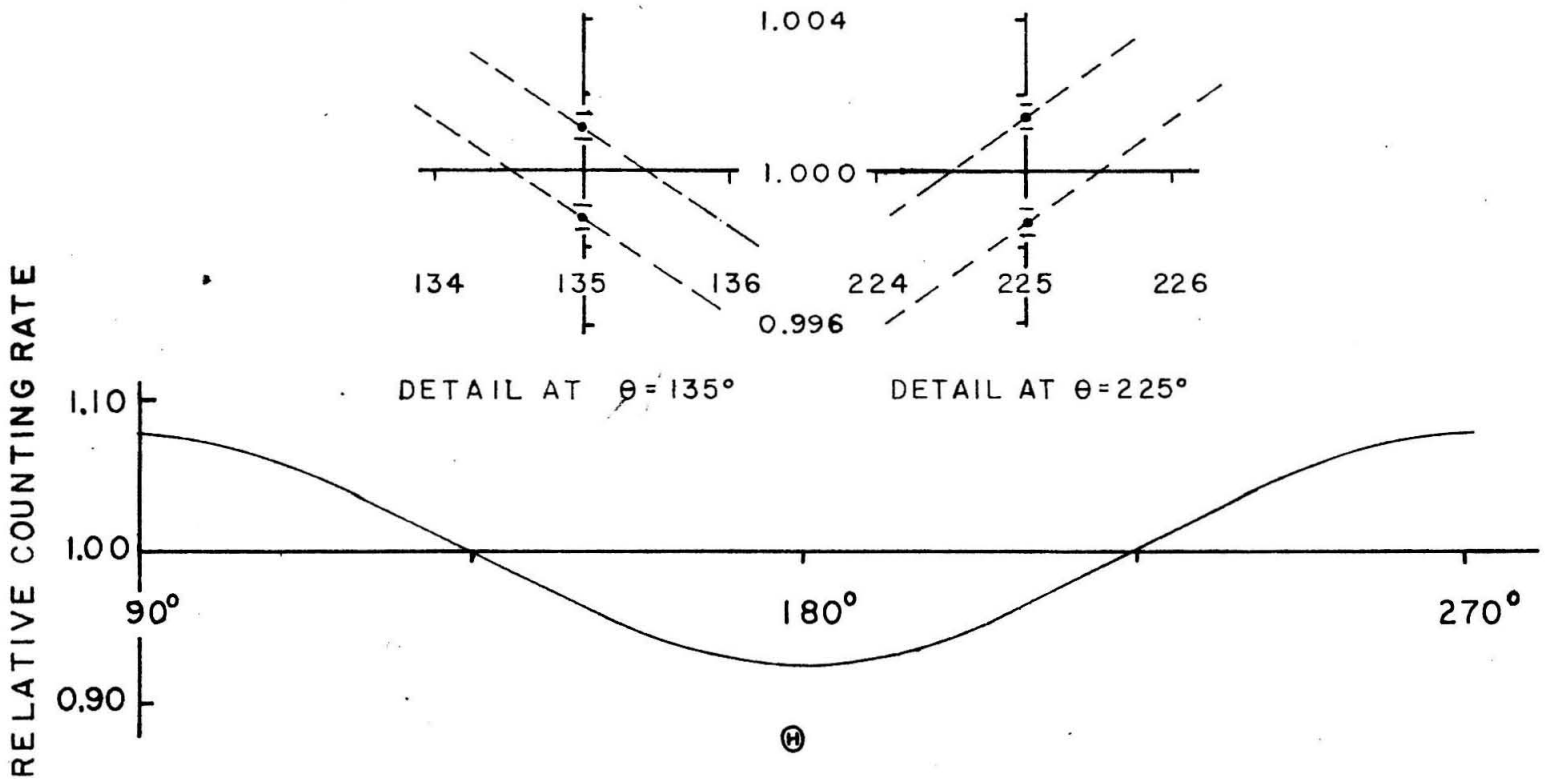

Figure 3. A typical angular correlation measurement. The curve shown is the average obtained for Hf^{177} (see section 4.5). The area around 135° and 225° is shown expanded to see the effect of switching the magnetic field up and down. The observed counting rate for each field direction is shown.

ment of the change in counting rate at one fixed angle for a reversal of the applied field (i. e., measurement of R). The electronic equipment used for both parts was the same. It consisted of a conventional fast-slow coincidence arrangement with a resolving time of $\sim 2 \times 10^{-8}$ sec. The NaI (Tl) crystals used were $1\frac{1}{2}$ inches in diameter. One was 2 inches long, and the other $1\frac{1}{2}$ inches long. They were mounted directly on RCA 6655 A photomultiplier tubes without the use of light pipes. The photomultipliers were shielded from magnetic fields by two layers of Netic and Co-Netic shielding. *

The system used for taking data was that the spectrum from one counter in coincidence with a narrow range of pulse heights from the other counter was recorded in a PENCO PA-4 pulse height analyzer. ** The instrument was used as a 50-channel analyzer with two sets of storage. For the angular correlation measurements, two angles were studied alternatively, the spectrum at one angle being stored in one memory array and the spectrum at the other angle being stored in the second memory array. (If more than two angles were studied, separate runs were made for pairs of angles.) The equipment was run automatically with alternate short counting periods at each of the two angles. A pair of scalers was also switched automatically to sum separately, at each angle, the total counts in the narrow pulse height range accepted from one of the counters. The counting time at each angle was also automatically summed. The

---

* Made by Perfection Mica Company, Illinois.

** Made by Pacific Electro-Nuclear Company, California.

same arrangement was used for the g-factor measurement, one set of storage being used for the field up, and the second for the field down. The use of automatic interchange between two counting arrangements enables a single measurement to be broken down into many hundreds of alternate counting periods, and hence effectively eliminated errors due to small changes in gain or efficiency of parts of the system.

The concept of these g-factor measurements was to design a magnet to minimize the leakage fields and then to run it at a sufficiently low field to ensure that all of its iron was in a region of high permeability. Figure 4 shows a sketch of the magnet and one of the counters. The flux return path for the magnet was a hollow cylinder around the coils and poles. A slot was cut in the cylinder to accept the conical lead shields for the scintillation counters. With this arrangement, and a field of 12,000 gauss in the 1/8" gap between the poles, the largest leakage field just outside the magnet was kept to a small fraction of a gauss. It was not necessary to use light pipes to remove the photomultiplier tubes from the vicinity of the magnet. The counters were set at the value of θ required and their change in gain, when the magnet was reversed, was measured. This was repeated for several rotations of the counters about their own axis. A position was found for each counter at which the gain change reversed sign. The counters were thus set to minimize the effects of the magnetic field. The maximum gain change for either counter was less than 1%, and at the rotation used was less than 0.05%. This procedure could be adopted for any angle θ between the two counters.

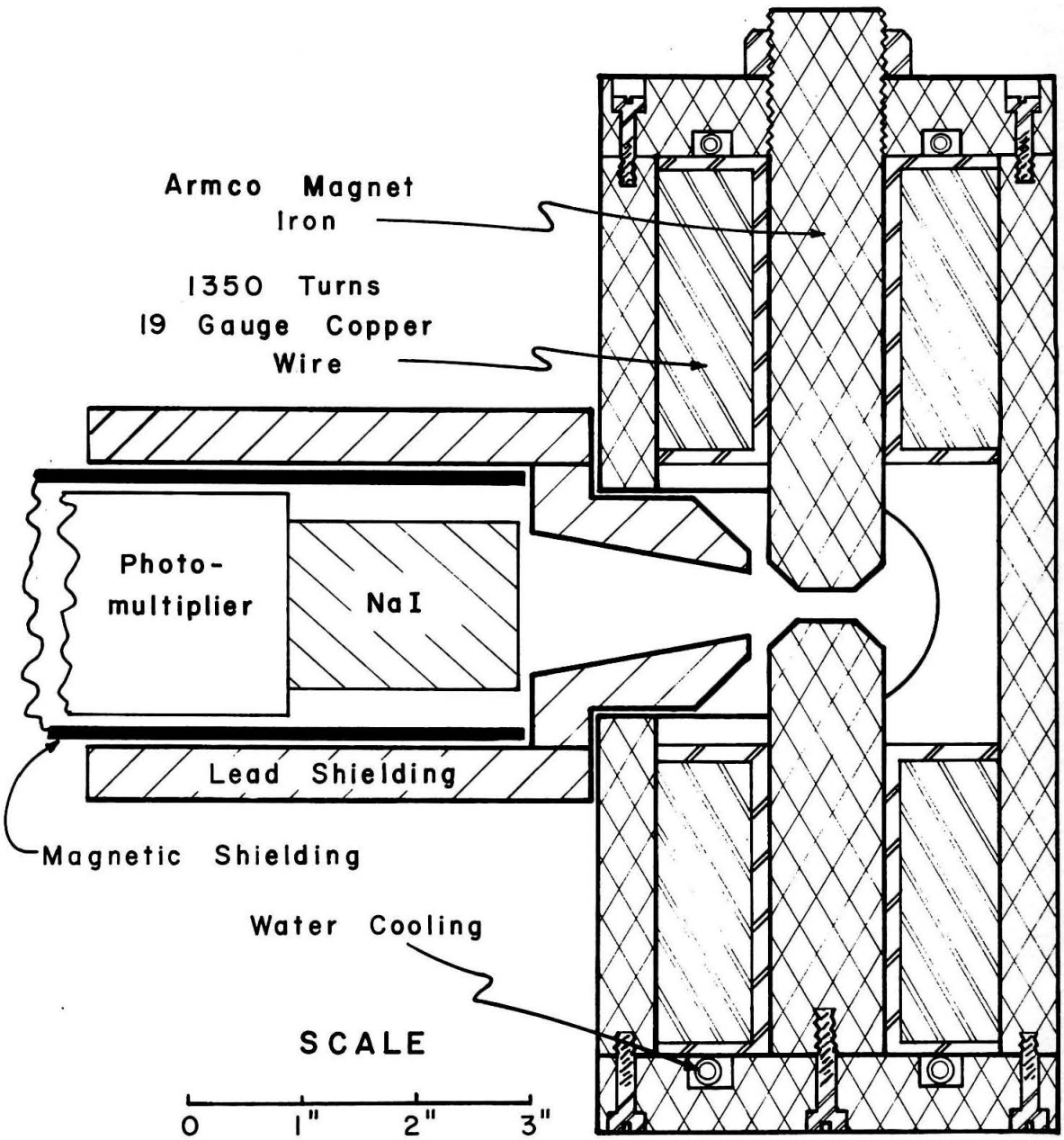

Figure 4. Section through magnet and one counter.

It was essential to reduce systematic effects resulting from reversal of the magnetic field, as the rotations of the angular correlation patterns to be measured were extremely small. A continual check on these systematic magnetic field effects was maintained throughout the experiment. For each direction of the field, the coincidence spectra from one counter were recorded, together with the summed counts within the small range of pulse heights accepted from the other counter.

The counters used had lead collimators to reduce spurious effects due to γ-ray scattering between the crystals. These collimators allowed a 1 1/4 inch diameter entrance aperture to the crystals at a distance of 2 1/2 inches from the source. With this arrangement, the finite solid angle correction for the counters required that the observed $P_2(\cos\theta)$ and $P_4(\cos\theta)$ coefficients, after correction for randoms, be multiplied by 1.10 ± 0.01 and 1.34 ± 0.04, respectively. As the effects to be measured were small, a large number of coincidence counts were necessary in order to obtain the required accuracy. It was reasonable, in general, to run with a significant proportion of random coincidences, as the effect of these was easily calculated, and the increased statistical accuracy obtained in a given counting time more than compensated for slight uncertainties so introduced. The random coincidences were easily measured by adding a delay of $\sim 10^{-7}$ sec. in one of the signal leads to the fast coincidence unit.

IV. EXPERIMENTAL RESULTS

4.0 Introduction

In this section, a short subsection is devoted to the measurement of each state, discussing the experimental data and its comparison to previous results. The states discussed are the 280 kev level in As^{75}, the 91 kev state in Pm^{147}, the 118 kev state in Tm^{169}, the 114 kev state in Lu^{175}, the 113 kev state in Hf^{177}, the 122 kev state of Sm^{152}, the 123 kev state of Gd^{154}, the 87 kev state in Dy^{160}, and the 81 kev state in Er^{166}.

4.1 280 kev Level of As^{75}

The g-factor of the 280 kev state in As^{75} was measured using the 121 - 280 kev cascade from the 401 kev level to the ground state. Figure 5 shows the significant parts of the As^{75} level scheme.

The angular correlation of the 121 - 280 kev cascade has been measured by Schardt and Welker[6] using a solid source. They obtained $W(\theta) = 1 - (0.40 \pm 0.03) P_2(\cos\theta) - (0.14 \pm 0.17) P_4(\cos\theta)$. Kelly and Wiedenbeck[7], who do not state the form of their source, obtained $W(\theta) = 1 - (0.41 \pm 0.03) P_2(\cos\theta)$. Using dilute selenic acid, van den Bold, et al[8] obtained $W(\theta) = 1 - (0.466 \pm 0.02) P_2(\cos\theta)$. The difference in these results may in part be due to the use of solid sources, but may also be due to the difficulty that the 401 kev state decays as well through a 136 - 265 kev cascade which is not completely resolved from the 121 - 280 kev cascade in any of the above experiments. All three of the above authors also deter-

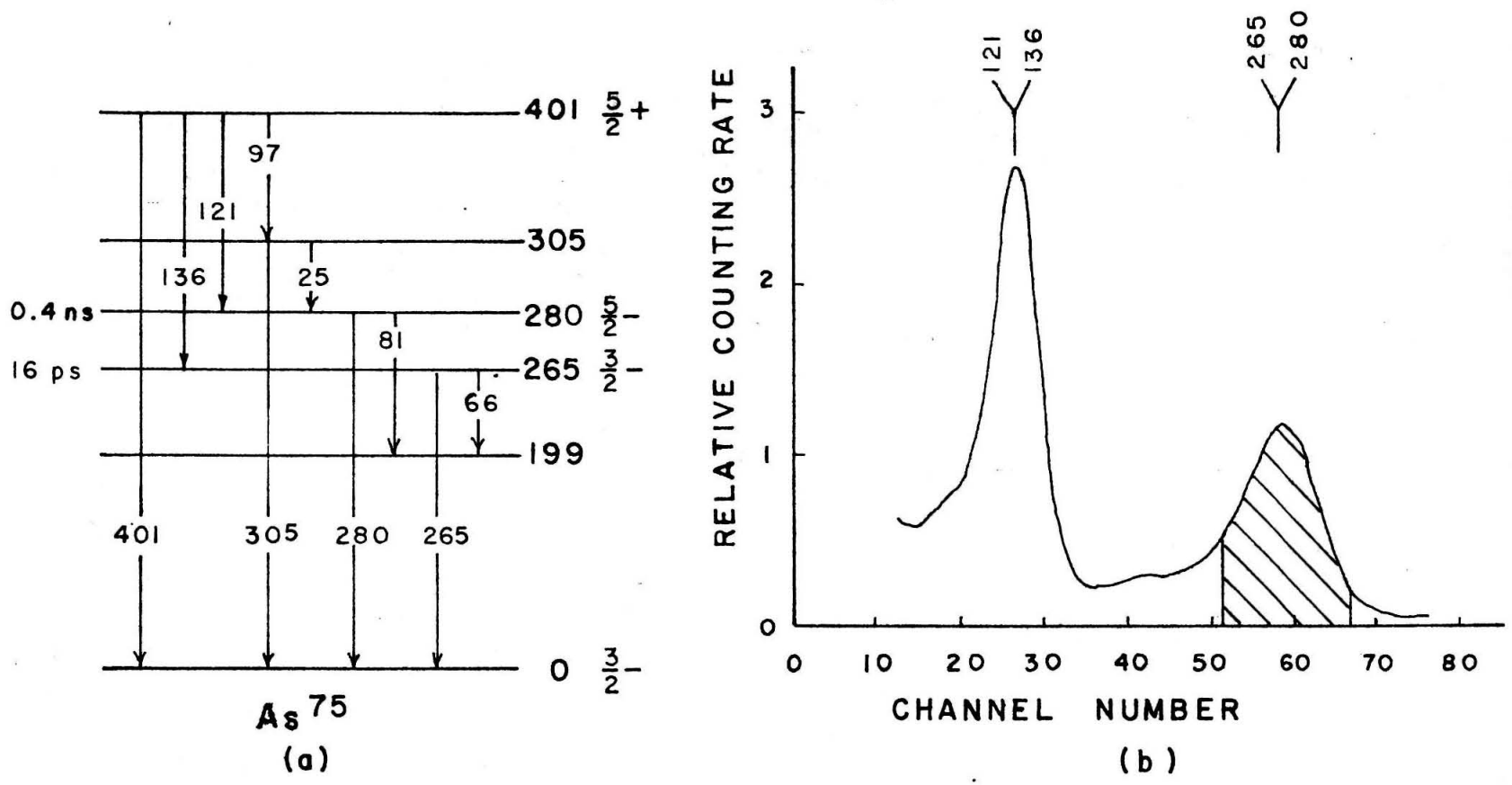

Figure 5. Level structure of As ^{75} and the pulse height spectrum of the Se ^{75} decay. Energies are in kev, and the mean lifetimes of the 280 kev and 265 kev states are shown. The cross hatched area shows the setting of the narrow gate.

mined the angular correlation for the 136 - 265 kev cascade. The results were $W(\theta) = 1 - (0.19\ ^{+0.01}_{-0.02})\ P_2(\cos\theta) - (0.012 \pm 0.012)\ P_4(\cos\theta)$, $W(\theta) = 1 - (0.016 \pm 0.030)\ P_2(\cos\theta)$ and $W(\theta) = 1 - (0.011 \pm 0.009)\ P_2(\cos\theta)$, respectively.

The source used for this measurement was a dilute nitric acid solution of neutron irradiated selenium metal enriched in Se^{74}. Since the 121 - 280 kev cascade was not well resolved from the 136-265 kev cascade, the measurement was made using the whole of both composite peaks. Figure 5 shows the pulse height spectrum, and the setting of the narrow gate. This reduces the observed anisotropy, but does not affect the g-factor measurement, since the correlation for the 136 - 265 kev cascade is nearly isotropic and its rotation will be small because the lifetime of the 265 kev state ($\tau = 1.6 \times 10^{-11}$ sec.) is short [9] compared to that of the 280 kev state. The observed angular correlation was $W(\theta) = 1 - (0.056 \pm 0.003) \cos 2\theta$. When corrected for finite solid angle and random coincidences, this gave $W(\theta) = 1 - (0.10 \pm 0.01)\ P_2(\cos\theta)$. This value is in agreement within the quoted error with that obtained from the other measurements, if the relative strengths of the 121 - 280 kev and 136 - 265 kev cascades are taken as 28:95 as indicated by the γ-ray intensities of Edwards and Gallagher [10].

The g-factor measurement was done at angles of 135° and 225° in a field of 12,000 gauss. The coincidence counting rate for both the angular correlation experiments and the g-factor experiments was of the order of 100 counts per second. A total of 8×10^6 counts was obtained in the coincidence peak for each direction of the

magnetic field at each angle. The values of R obtained were (0.0023 ± 0.0005) and $-(0.0017 \pm 0.0006)$ for $\theta = 135^\circ$ and 225°, respectively. The average of these two measurements gives, using Eq. (20), $G\omega\tau = (1.72 \pm 0.34) \times 10^{-2}$ radians.

The lifetime of the 280 kev level of As^{75} has been measured to be $(4 \pm 1) \times 10^{-10}$ sec.[11] Since the angular correlation shows only a small difference between liquid and solid sources, $G_2 = 1$ is assumed for liquid sources. Since As^{75} does not have a large quadripole moment, and the nuclear lifetime is short, this is to be expected. Arsenic is not paramagnetic, and hence β is taken as 1. Using these values, we find

$$g = \frac{0.39 \pm 0.12}{\beta G} = 0.39 \pm 0.12 .$$

4.2 91 kev State of Pm^{147}

Figure 6 shows the level scheme of Pm^{147}. Two previous measurements of the g-factor for the 91 kev state in Pm^{147} have been reported. Lindquist and Karlsson[12] obtained an upper limit $g = 1$. Bodenstedt, et al[13] obtained a preliminary value of $g = (0.43 \pm 0.15)$. Both of these groups used the 321 - 91 kev cascade from the 412 kev state to the ground state.

Lindquist and Karlsson used a source of Nd_2O_3 dissolved in alcohol, and obtained an angular correlation of $W(\theta) = 1 - (0.097 \pm 0.007) P_2(\cos\theta) + (0.023 \pm 0.018) P_4(\cos\theta)$. They re-measured the angular correlation in a field of 25,000 gauss, and were able to place a limit on the g-factor only.

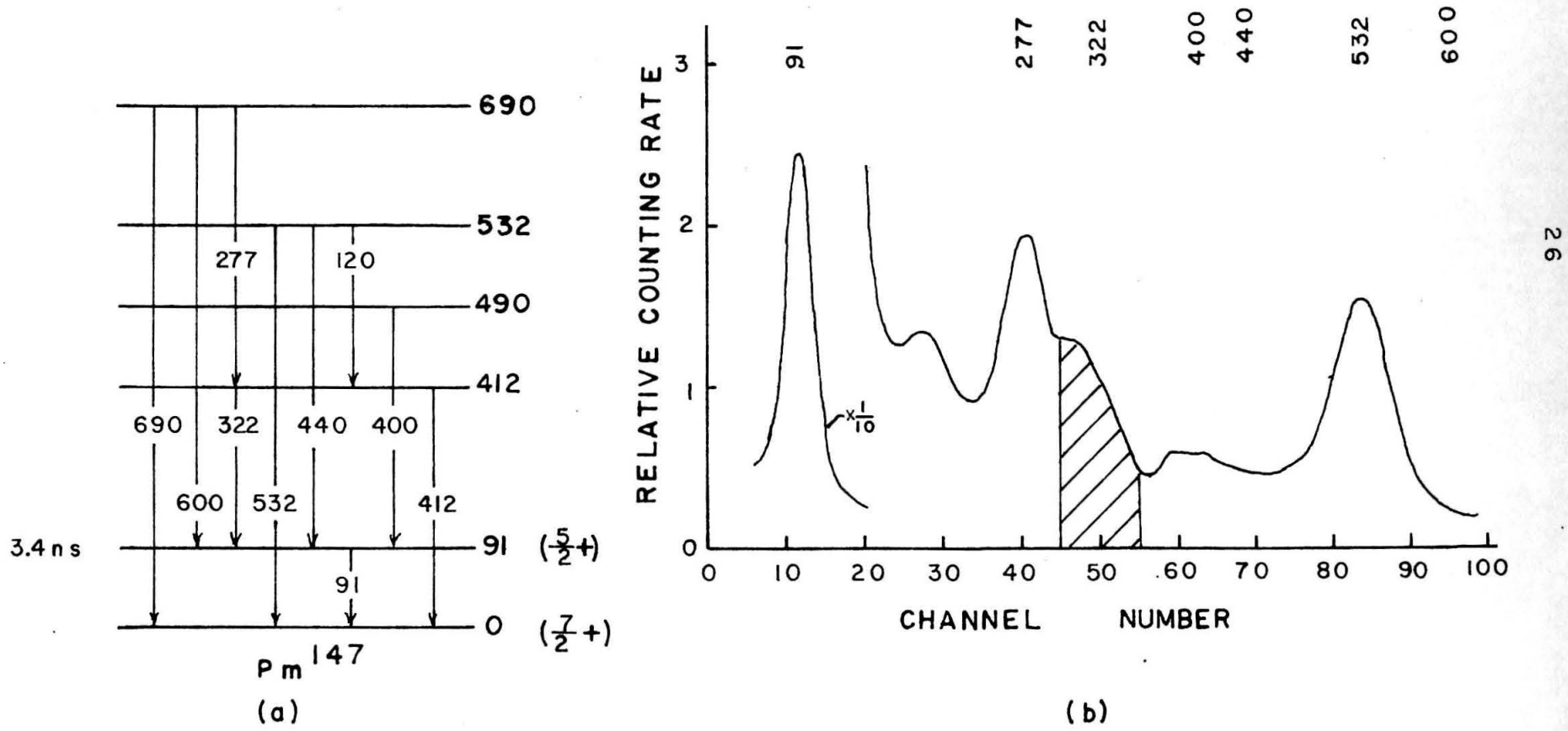

Figure 6. Level structure of Pm^{147}, and the pulse height spectrum of the Nd^{147} decay. The energies are in kev, and the mean lifetime of the 91 kev level is shown. The cross hatched area shows the setting of the narrow gate on the 322 kev line.

Bodenstedt, et al[13] used a saturated aqueous solution of Nd_2Cl_3 as source. They measured an angular correlation of $W(\theta) = 1 - (0.11 \pm 0.01) P_2(\cos \theta)$. The angular correlation was measured for each direction of a 37,200 gauss field, and the rotation calculated, from which the preliminary value quoted above was obtained. They do not state that they have applied a paramagnetic correction to their results. Their measurement was somewhat hampered by poor energy resolution of the counters.

We measured the g-factor of the 91 kev state using the 321 - 91 kev cascade as well. The source was Nd_2O_3 dissolved in alcohol. Figure 6 shows the pulse height spectrum and the setting of the narrow gate. Our observed angular correlation was $W(\theta) = 1 - (0.025 \pm 0.003) \cos 2\theta$, which, when corrected for solid angle and random coincidence counts, gave $W(\theta) = 1 - (0.042 \pm 0.005) P_2(\cos \theta)$. The measurements were made at five angles between 90° and 180°, and showed no significant $P_4(\cos \theta)$ term.

The g-factor was measured at $\theta = 135^\circ$ in a field of 12,000 gauss. The 91 kev γ-ray is K-converted and the x-ray peak in coincidence with the 320 kev γ-ray was used as a check on the measurement. About 10^5 counts were observed in the coincidence peak for each field direction. A value of $R = (0.031 \pm 0.004)$ was observed for the 321 - 91 kev cascade, while $R = (0.002 \pm 0.005)$ was observed for the K x-ray in coincidence with the 321 kev line. Equation (20) was used to evaluate $G_2 \omega\tau$ with the result,

$$G_2 \omega\tau = -(0.38 \pm 0.09) \text{ radians.}$$

The lifetime of the 91 kev state has been measured to be $(3.4 \pm 0.1) \times 10^{-9}$ sec.[14] The paramagnetic correction factor β is predicted in Appendix I to be 2.1. Bodenstedt, et al measured the angular correlation with a delay of 2 half-lives, and concluded that the time dependent attenuation was small. However, since the angular correlation results we obtained are not in agreement with the other measurements, it is difficult to assert that $G_2 = 1$. Using the known values of the parameters, Eq. (20) gives

$$g = \frac{(1.95 \pm 0.4)}{\beta G_2} = \frac{(0.93 \pm 0.20)}{G_2} .$$

G_2 is probably between 0.5 and 1.0.

4.3 118 kev State of Tm^{169}

The level scheme of Tm^{169} below the 316 kev state is shown in Fig. 7. The 198 - 110 kev cascade from the 316 kev level in Tm^{169} was used to measure the g-factor of the 118 kev state. The angular correlation of the 198 - 110 kev cascade has been measured by Cappellar and Klingelhöfer[15], and by Koicki, Simic and Kucoc[16]. The first-mentioned authors used an oxide source and found $W(\theta) = 1 + 0.250\, P_2(\cos\theta) + 0.029\, P_4(\cos\theta)$. The second group, using $YbCl_3$ in a dilute HCl solution as a source, obtained $W(\theta) = 1 + (0.314 \pm 0.003)\, P_2(\cos\theta) + (0.003 \pm 0.005)\, P_4(\cos\theta)$. Cappelar and Klingelhöfer measured the angular correlation with a delay between γ_1 and γ_2 of 4×10^{-9} seconds and observed no significant at-

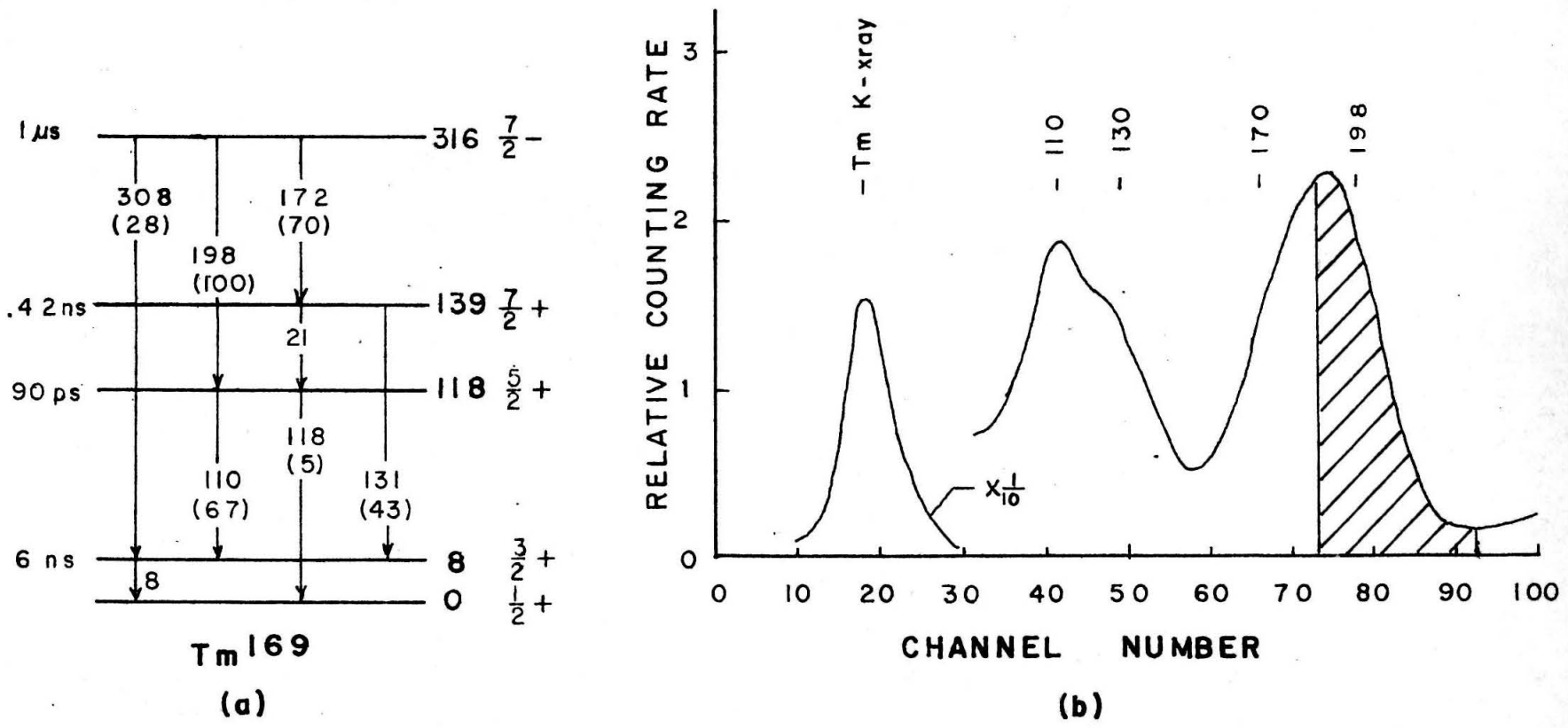

Figure 7. Level structure of Tm^{169} below the 316 kev level and the corresponding part of the pulse height spectrum of the Yb^{169} decay. Energies are shown in kev, and the mean lifetime of the states are given. Relative γ-ray intensities are shown in parenthesis. The cross hatched area shows the setting of the narrow gate.

tenuation. The discrepancy in the two angular correlations may possibly result from the difficulty of resolving the 198 - 110 kev cascade from the 177 - 130 kev cascade and the 177 - 110 kev coincidences through the intermediate 21 kev γ-ray.

Our measurements were done using a source of neutron irradiated Yb_2O_3 dissolved in dilute nitric acid. Figure 7 shows the pulse height spectrum of Tm^{169} and the setting of the narrow gate. The observed angular correlation was $W(\theta) = 1 + (0.155 \pm 0.005) \cos 2\theta$. This, when corrected for random coincidences and finite solid angle of the counters, gave $W(\theta) = 1 + (0.28 \pm 0.01) P_2(\cos \theta)$. The interference from the 177 - 130 kev and 177 - 110 kev coincidences can be estimated from the data of Koicki, et al, and the intensity of the 130 kev peak in the coincidence spectrum. It was found that the 177 - 110 kev and the 177- 130 kev coincidences were $\sim 2.5\%$ and 1% respectively of the 198 - 110 kev coincidences with the settings used. The angular correlation between the 198 kev γ-rays and the lower half of the 110 kev peak collected by the pulse height analyzer yielded results in agreement with those of Koicki, et al, after corrections for random coincidences and finite solid angle of the counters.

The g-factor measurement was made at an angle of 135° in a field of 12,000 gauss. 3×10^6 counts were observed in the 110 kev coincidence peak for each direction of the field. The K x-ray peak in coincidence with the 198 kev γ-ray was observed to check that no systematic error was present. The value of R observed for the

198 - 110 kev cascade was R = (0.32 ± 0.10) %. The value of R observed for the 198 kev - K x-ray coincidence peak was R = (0.02 ± 0.06) %. Using Eq. (19), one can calculate from this, $G_2\omega\tau$ = (0.56 ± 0.17) x 10^{-2} radians.

Blaugrund[17] has measured the lifetime of the 118 kev state to be τ = (9.0 ± 1.5) x 10^{-11} sec. The delayed coincidence measurement of Cappelar and Klingelhofer cited above supports the prediction that G_2 should be unity for such a short lifetime. β is estimated in Appendix I to be 5.6.*

Because the lifetime of the 138 kev level is significantly longer than that of the 118 kev level (4.0 x 10^{-10} sec. and 9.0 x 10^{-11} sec., respectively)[17], a small admixture of the 177 - 130 kev cascade could have a large enough rotation to affect the results significantly. Using the admixtures quoted above and a theoretical value of g = 0.2 for the 139 kev state, as predicted by the Nilsson model[13] one finds that this effect can at the most decrease the observed g by 10% , and is probably considerably less. This is not included in the quoted error.

Using the values quoted for the relevant parameters in Eq. (20), one obtains

$$g = \frac{1.2 \pm 0.4}{G_2\beta} = 0.21 \pm 0.07.$$

---

* Although the large disturbance of the electronic configuration makes the calculation of β difficult for cascades preceded by a K-capture, the 1 microsec lifetime of the 316 kev level in Tm^{169} from which all these cascades are fed should allow sufficient time for electronic reorganization to justify this value.

4.4 114 kev State of Lu^{175}

The level scheme of Lu^{175} is shown in Figure 8. The g-factor of the 114 kev state of Lu^{175} was measured using the 282 - 114 kev cascade from the 396 kev level to the ground state.

The angular correlation of the 282 - 114 kev cascade has been studied by Klema[19] and by Wiedling[20]. Klema obtained $W(\theta) = 1 + (0.221 \pm 0.004) P_2 (\cos \theta)$ for a liquid source, and $W(\theta) = 1 + (0.210 \pm 0.003) P_2 (\cos \theta)$ for a solid source. Wiedling measured the correlation for aqueous solutions of $Yb_2(NO_3)_3$ with and without glycerine added. He obtained $W(\theta) = 1 + (0.227 \pm 0.004) P_2 (\cos \theta)$ independent of viscosity. These results indicate that quadripole attenuation of this correlation is small for liquid sources.

Our measurements were made using two different sources of neutron irradiated Yb^{174} oxide dissolved in dilute nitric acid. The observed angular correlations were $W(\theta) = 1 + (0.107 \pm 0.002) \cos 2\theta$ and $W(\theta) = 1 + (0.167 \pm 0.020) \cos 2\theta$ for the first and second runs, respectively. Random coincidence rates varied from 30% to 10% for Run 1, and from 10% to 5% in Run 2, as the source decayed. The above angular correlations corrected for finite solid angle and random coincidences resulted in $W(\theta) = 1 + (0.200 \pm 0.003) P_2 (\cos \theta)$, $W(\theta) = 1 + (0.21 \pm 0.03) P_2 (\cos \theta)$ for Runs 1 and 2 respectively. The rotation measurements were done at 135° in a field of 12,000 gauss. In each run, over 4×10^6 counts were observed in the x-ray and γ-ray coincidence peaks for both directions of the magnetic field. The value of R obtained for the γ-ray was $R = 0.15\% \pm 0.09\%$ for

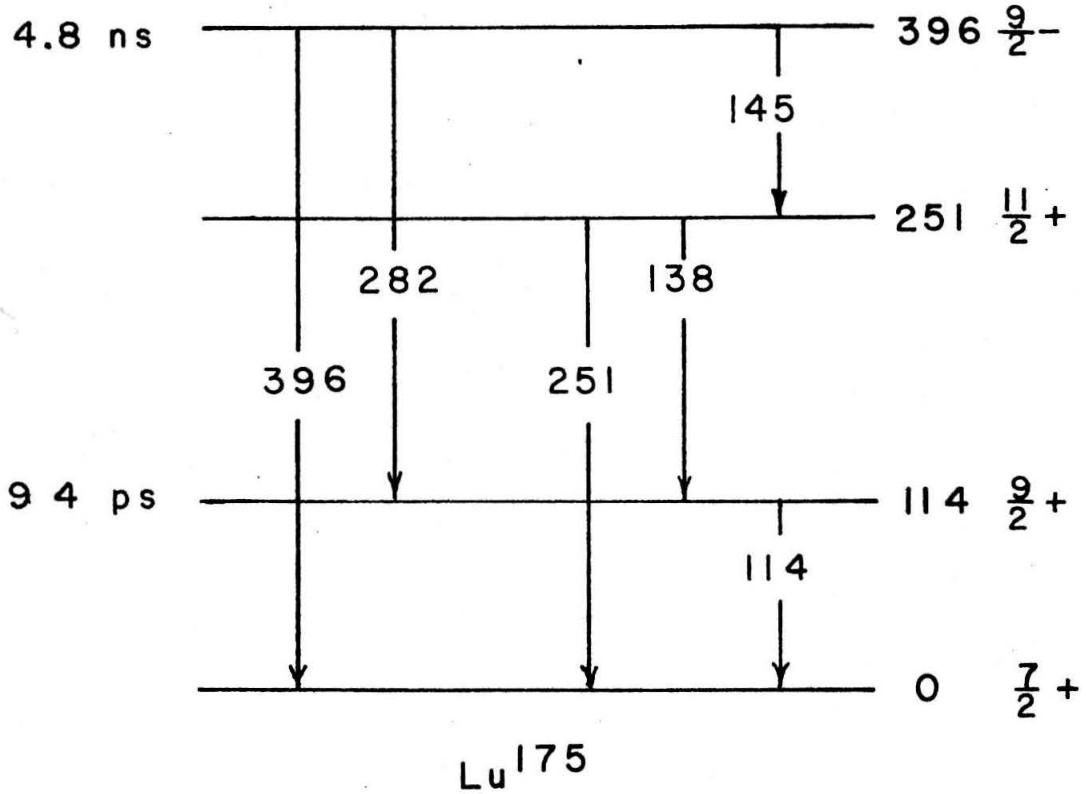

Figure 8. Level structure of Lu^{175}. The energies are in kev and the mean lifetimes of the 396 kev state and the 114 kev state are shown.

Run 1 and R = 0.23% ± 0.10% in Run 2. For the x-ray, we found R = - 0.02% ± 0.06% and R = - 0.07% ± 0.06% , respectively. The above results for the γ-ray are normalized on the x-ray, and the error included both γ-ray and x-ray counting errors.

Using Eq. (20) of Section 3.0, we obtain for the two runs, $G\omega\tau = (0.35 \pm 0.17) \times 10^{-2}$ radians, and $G\omega\tau = (0.35 \pm 0.12) \times 10^{-2}$ radians.

The lifetime of the 114 kev state can be calculated using the Coulomb excitation data from the compilation of Alder, et al[21]. Using the value $\delta^2 = 0.22$ for the E2/M1 intensity ratio obtained by Martin, et al[22], one obtains a mean life of $\tau = 9.4 \times 10^{-11}$ sec.

From the evidence of the angular correlation work quoted above, G_2 is taken to be 1. β should be 1 for Lu, since it is not paramagnetic, and therefore we obtain

$$g = \frac{0.65 \pm 0.25}{G\beta} = 0.65 \pm 0.25 \quad .$$

4.5 113 kev State of Hf^{177}

The level scheme of Hf^{177} is shown in Fig. 9. The cascade used to measure the g-factor of the 113 kev state in Hf^{177} was the 208 - 113 kev cascade from the 321 kev level to the ground state. The 321 kev level is populated by β decay from 6.8-day Lu^{177}.

Several authors have measured the angular correlations of the 208 - 113 kev cascade. Wiedling[23] measured the correlation for liquid sources of various viscosity and concluded that the undisturbed correlation is $W(\theta) = 1 - (0.163 \pm 0.002) P_2(\cos\theta) + (0.002$

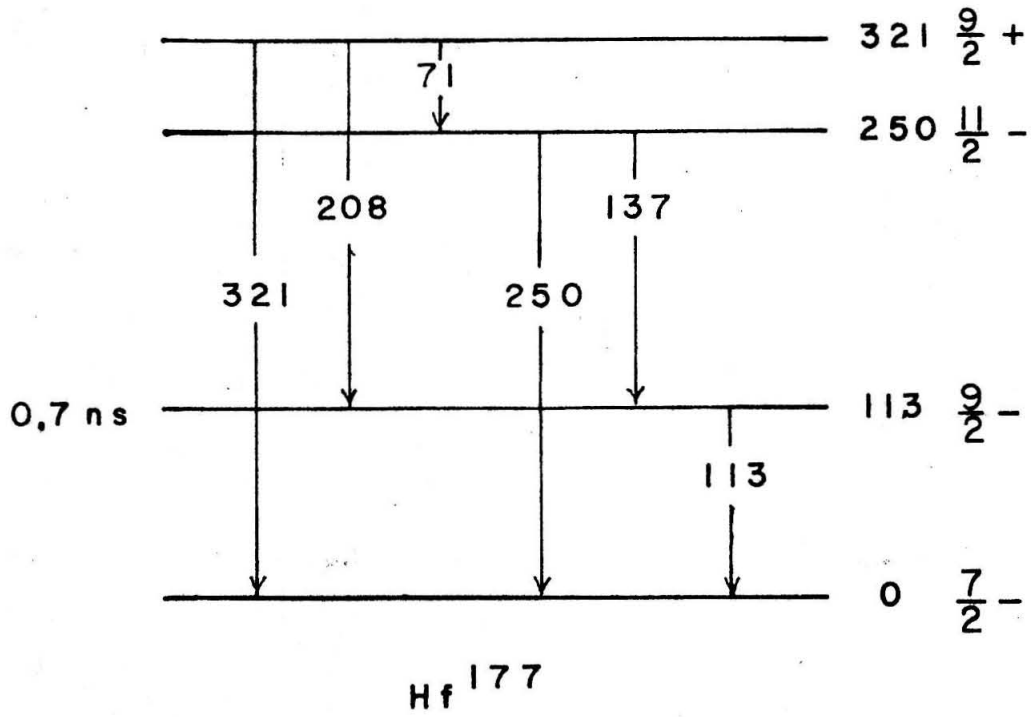

Figure 9. Level structure of Hf^{177}. The energies are in kev and the mean lifetime of the 113 kev level is shown.

$\pm$ 0.002) P_4 (cos θ). For dilute aqueous sources he obtained $W(\theta) = 1 - (0.160) P_2(\cos\theta)$. Ofer[24] found $W(\theta) = 1 - (0.135 \pm 0.010) P_2$ (cos θ) for aqueous sources. Klema[25] measured the correlation for solid and liquid sources, obtaining $W(\theta) = 1 - (0.149 \pm 0.002) P_2(\cos\theta)$ and $W(\theta) = 1 - (0.1614 \pm 0.0015) P_2(\cos\theta)$, respectively. Behrend[26] obtained the correlation for $LuCl_3$ in aqueous solution, in aqueous solution with glycerine added, and in a solid form. He found $P_2(\cos\theta)$ coefficients of - (0.1627 $\pm$ 0.0032), - (0.1511 $\pm$ 0.0027), and - (0.1311 $\pm$ 0.0023), respectively.

The source used in our experiment was neutron irradiated Lu_2O_3 dissolved in dilute nitric acid. The angular correlation after correction for random coincidences and finite solid angle of the counters was $W(\theta) = 1 - (0.16 \pm 0.015) P_2(\cos\theta)$.

The g-factor was measured at angles of 135° and 225° in a field of 12,000 gauss. The values of R found for x-ray and γ-ray coincidences, and the observed coefficient of cos 2θ in the angular correlation, are given in Table 1. A total of 1.2×10^7 counts was observed in the 113 kev γ-ray coincidence peak for each direction of the field. The coincidence counting rate varied from 200 to 100 counts per second, and the random rate from 20% to 10% as the source decayed. The value of $G_2\omega\tau$ calculated from Eq. (20) was - (0.0091 $\pm$ 0.0014) radians.

The lifetime of the 113 kev level has been measured by Berlovich[27] to be 6×10^{-10} sec. Hauser, et al[28] have found $\tau = (7.2 \pm 0.7) \times 10^{-10}$ sec. $\tau = 7 \times 10^{-10}$ sec. is used for the evaluation of g. Since neither Hf nor Lu is paramagnetic, β should be

TABLE 1

RESULTS FOR MEASUREMENTS ON THE 113-kev STATE OF Hf^{177}

θ	R for 208 keV X-ray coincidences	R for 113-208 keV coincidences	average value of C_2 for 208-113 keV cascades	$G_2\omega\tau$
135°	-(0.0002±0.0007)	+(0.0024±0.0006)	-0.070	-(0.0086±0.0021)
225°	-(0.0005±0.0007)	-(0.0031±0.0006)	-0.081	-(0.0095±0.0019)
			average value	-(0.0091±0.0014)

unity. The angular correlation measurements in liquid sources indicate $G_2 = 1$. Using these values, we find

$$g = \frac{0.20 \pm 0.06}{\beta G} = 0.20 \pm 0.06 .$$

4.6 122 kev State of Sm^{152}

The level scheme of Sm^{152} is shown in Fig. 10. The g-factor of the 122 kev state of Sm^{152} has been measured by Goldring and Scharenberg[29] and by Sugimoto[30]. Goldring and Scharenberg used a liquid source of $Sm_2(NO_3)_3$ and populated the 122 kev state by Coulomb excitation using protons. After correcting their results for the effects of paramagnetism, they obtained $g = 0.21 \pm 0.04$. Sugimoto, using the same method, found $g = (0.36 \pm 0.16)/\beta G$ (in our notation) using a solid oxide source at 700°K.

Our measurement was done using the 1,420 - 122 kev cascade from the 1,540 kev level to the ground state. The 1,540 kev level was populated by a K-capture transition in Eu^{152}. The angular correlation for this cascade has been measured by Hartman and Wiedling[31], and by Ofer[32]. Hartman and Wiedling used aqueous solutions of $EuCl_3$ and obtained $W(\theta) = 1 + (0.219 \pm 0.005) P_2(\cos\theta) + (0.003 \pm 0.007) P_4(\cos\theta)$. Ofer used a dilute solution of $Eu_2(SO_4)_3$ as a source and obtained $W(\theta) = 1 + (0.21 \pm 0.02) P_2(\cos\theta) + (0.02 \pm 0.03) P_4(\cos\theta)$.

The source for our measurements was neutron irradiated Eu_2O_3, enriched in Eu^{151}, dissolved in dilute nitric acid. The observed angular correlation was $W(\theta) = 1 + (0.142 \pm 0.004) P_2(\cos\theta)$,

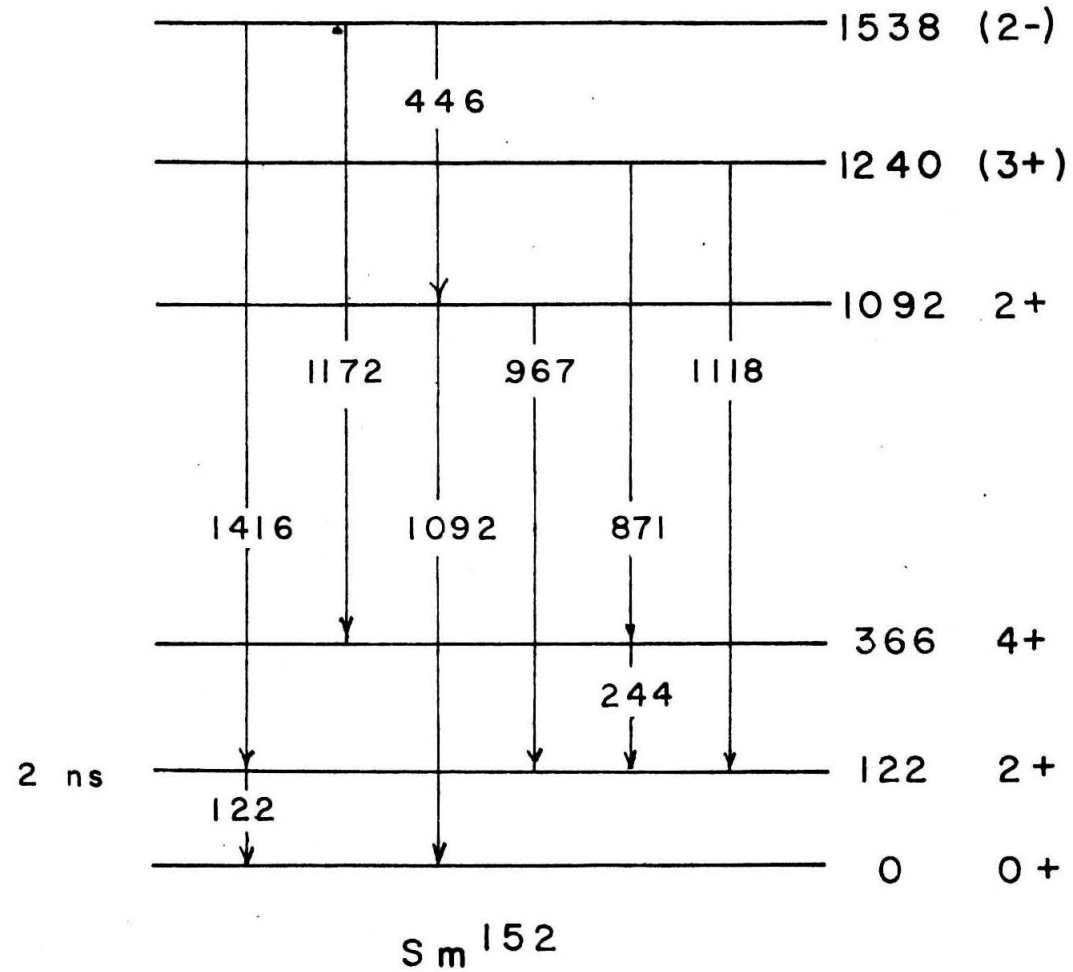

Figure 10. Level structure of Sm^{152}. Energies are in kev. The mean life of the 122 kev level is given.

which after correction for random coincidences and finite solid angle of the counters gave $W(\theta) = 1 + (0.205 \pm 0.007) P_2(\cos\theta)$. This is in reasonable agreement with the results of Hartman and Wiedling, and Ofer.

The g-factor measurement was done at an angle of 135° in a field of 12,000 gauss. A total of 2.5×10^5 counts was observed in the coincidence peak corresponding to the 1,420 - 122 kev coincidences. The coincidence peak corresponding to the 1,420 kev — K x-ray coincidences resulting from K-conversion of the 221 kev γ-ray was also observed. The value of R observed for the 1,420 - 122 kev cascade was $(2.1 \pm 0.5)\%$, which gave $G_2 \omega\tau = (3.7 \pm 0.9) \times 10^{-2}$ radians. The observed value of R for the 1,420 kev — K x-ray cascade was $(0.0 \pm 0.2)\%$, which indicates no significant systematic effects.

The value of G_2 for the 122 kev level was measured by Goldring and Scharenberg for a liquid source by comparing the observed γ-ray distribution following Coulomb excitation to the theoretical prediction. They found $G_2 = 1$. We made a direct measurement of G_2 for the source used in the g-factor experiment by measuring the correlation for the 144 - 122 kev cascade. Since this is a cascade of two pure E2 γ-rays, the theoretical value for the cascade is known. The observed angular correlation was corrected for contributions from tails of other γ-rays by measuring the correlation with a narrow gate set just above and just below the 144 kev γ-ray. The value obtained was $G_2 = 1.0 \pm 0.13$. The lifetime of the 122 kev state has been measured as $\tau = (2.0 \pm 0.14) \times 10^{-9}$ sec.[33]

The value of β predicted for the Sm^{3+} ion in Appendix I is $\beta = 1.15$. The rather sizable difference between this value and the value of $\beta = 1.7 \pm 0.2$ used by Goldring and Scharenberg arises from the sizable contribution of second order terms in the calculation of this quantity for the Sm^{3+} ion (see Kanamori and Sugimoto[34], and Appendix I).

Using the values from above in Eq. (20), our experimental results yield

$$g = \frac{(0.32 \pm 0.08)}{\beta G} = 0.28 \pm 0.07 .$$

This can be compared to the value of $g = 0.30 \pm 0.06$ obtained from Goldring and Scharenberg's work with the more accurate paramagnetic correction factor, and the value of $g = 0.34 \pm 0.16$ obtained from Sugimoto's work using $G_2 = 1$, $\beta = 1.07$ (see Ref. 34). The agreement between these different measurements is most pleasing in light of the different methods used to populate the 122 kev level, and furnishes some support for the assumption that the ion containing the radioactive nucleus has reached an equilibrium state in a time short compared to the nuclear lifetime.

4.7 123 kev State of Gd^{154}

The g-factor of the 123 kev state of Gd^{154} was measured using the 1,280 - 123 kev cascade from the 1,400 kev state. The 1,400 kev state was populated by β decay from 16-year Eu^{154}. The level scheme of Gd^{154} is shown in Fig. 11.

The angular correlation of the 1,280 - 123 kev cascade has

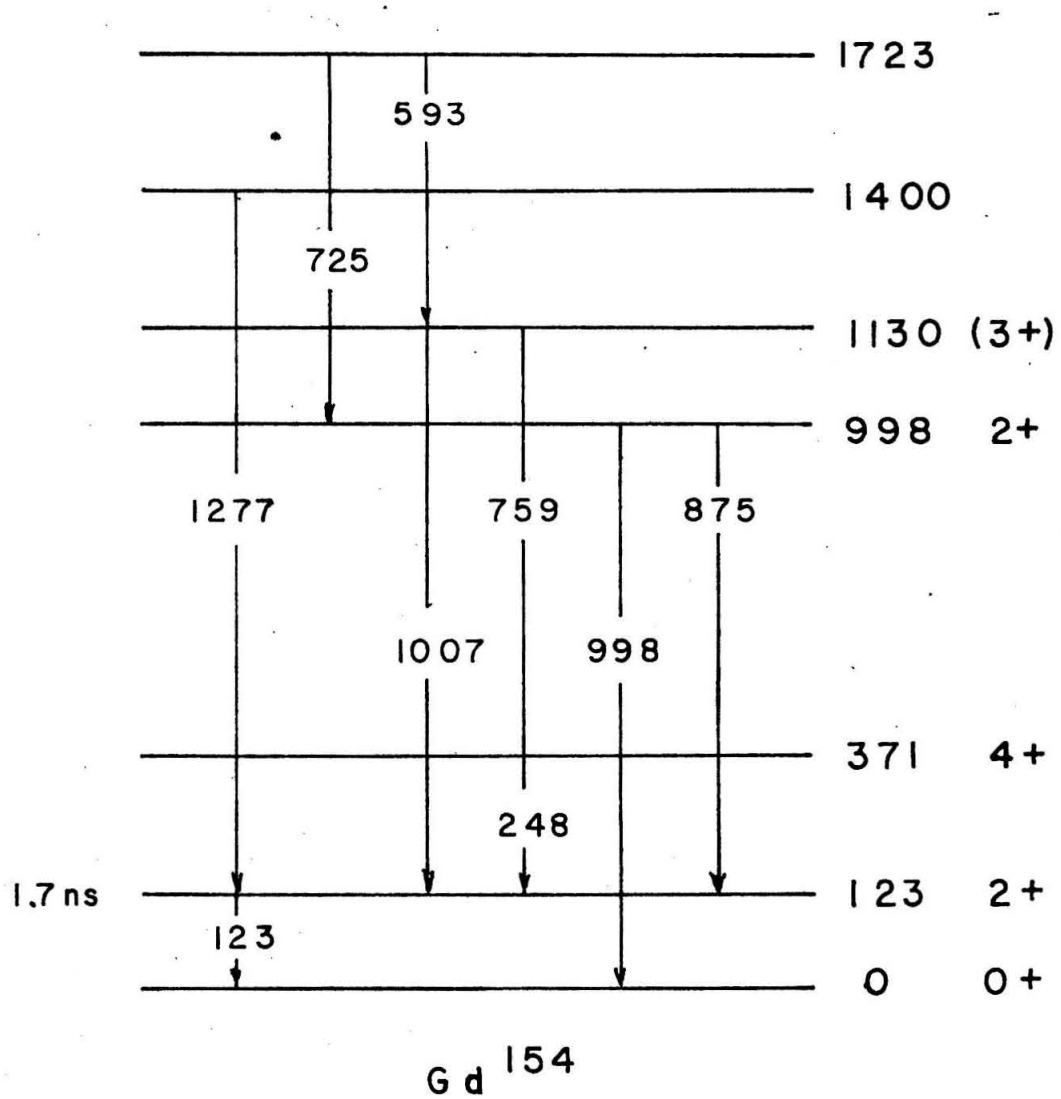

Figure 11. Level structure of Gd^{154}. The energies are shown in kev. The mean lifetime of the 123 kev state is indicated.

been measured by Hickman and Wiedenbeck[35]. They used a source of Eu_2O_3 dissolved in dilute HCl, and obtained an angular correlation of $W(\theta) = 1 + (0.19 \pm 0.010) P_2(\cos\theta) - (0.007 \pm 0.015) P_4(\cos\theta)$. These authors also measured the correlation of the 248 - 123 kev cascade from the 371 kev state. They obtained $W(\theta) = 1 + (0.098 + 0.018) P_2(\cos\theta) - (0.020 \pm 0.024) P_4(\cos\theta)$. This result is in good agreement with that expected for a (4(Q)2(Q)0) cascade. The attenuation coefficient for the 123 kev level calculated from these results is $G_2 = 0.96 \pm 0.18$. Goldring and Scharenberg[29] also have measured the attenuation coefficient for the 123 kev state of Gd^{154} in a dilute nitric acid solution by comparing the theoretical angular distribution of γ-rays from a Coulomb excited 2+ state with that observed experimentally. The result was $G_2 = 0.5 \pm 0.06$. They have measured the attenuation for similar states in Gd^{156} and Gd^{160} and conclude that the observed effect results from a static magnetic hyperfine attenuation rather than electric quadripole interaction. Deutsch and Stiening[36] have shown that this explanation is,in fact, correct, by demonstrating that the attenuation of the 1,280 - 123 kev cascade can be removed by application of a small magnetic field parallel to the axis of one of the detectors.

As this experiment demonstrates, attenuation resulting from static magnetic hyperfine interaction is not independent of the value or direction of the applied field. It can be removed with a strong enough field applied along the direction of one of the γ-rays, or increased considerably by a field perpendicular to the plane of the correlation measurements.

We have measured the angular correlation of the 1,280 - 123 kev cascade using a source of neutron irradiated Eu_2O_3 enriched in Eu^{153}, which was dissolved in dilute nitric acid. The observed correlation after correction for finite solid angle and random coincidences was $W(\theta) = 1 + (0.170 \pm 0.008) P_2 (\cos \theta)$. We also measured the correlation of this cascade in a magnetic field of 12,000 gauss. We found $W(\theta) = 1 + (0.059 \pm 0.006) P_2 (\cos \theta)$ after correction for random coincidences and finite solid angle. The attenuation coefficient in zero field was determined by measuring the angular correlation of the 248 - 123 kev (4(Q)2(Q)0) cascade, whose theoretical value is known. Interference from competing cascades was corrected for by measuring the correlation with the gate set just above and just below the 248 kev line. The result was $W(\theta) = 1 + (0.075 \pm 0.015) P_2 (\cos \theta)$, which gave an attenuation coefficient of $G_2 = 0.74 \pm 0.15$. The angular correlation observed for the 1,280 - 123 kev cascade is consistent with that of Hickman and Wiedenbeck when corrected by this factor.

In Section 2.3 and Appendix I, static magnetic hyperfine attenuation is shown to be an expected property of the Gd^{3+} ion. The observation of magnetic hyperfine attenuation therefore furnishes strong evidence that the equilibrium electronic configuration has been reached in a time short compared to the nuclear lifetime. It is somewhat difficult to understand the results of Hickman and Wiedenbeck on the basis of the above evidence, since, although they used a different source material, one would not expect that the relaxation time would be markedly different. If these results are indeed correct, then the

g-factor could be measured much more accurately in a solution of $EuCl_3$ than in a solution of $Eu_2(NO_3)_3$.

The g-factor measurement itself was done at an angle of 135° in a field of 12,000 gauss. The observed angular correlation in the magnetic field was $W(\theta) = 1 + (0.039 \pm 0.010) \cos 2\theta$. The value of R obtained was $(0.20 \pm 0.25)^{o}/o$, which gives a value of $G_2 \omega\tau = (1.25 \pm 1.56) \times 10^{-2}$ radians.

The value of G_2 can be calculated from the observed attenuation in the magnetic field, and the measured value in zero field to be $G_2 = 0.24 \pm 0.05$. The lifetime has been measured to be $(1.7 \pm 0.14) \times 10^{-9}$ sec.[33] As pointed out in Appendix I, the calculation of a β for Gd^{3+} is not reasonable, since the assumption of thermal equilibrium is not correct. Therefore, $\beta = 1$ is used in the formulas. The g-factor is calculated on the assumption that the attenuation has the same time dependence as that of electric quadripole attenuation, which is a satisfactory approximation for the purposes of this work. The value of g obtained on this basis is

$$g = 0.4 \pm 0.5 \quad .$$

4.8 87 kev State of Dy^{160}

The level scheme for Dy^{160} is shown in Fig. 12. The g-factor of the 87 kev state has been measured by Debrunner, et al[37]. They observed the rotation of the angular correlation of the 800 - 87 kev cascade in a magnetic field using a solid Tb_2O_3 source containing Tb^{160}. The measurement was done at 300°K and allowed independent calculation of the paramagnetic correction factor, β, and the apparent

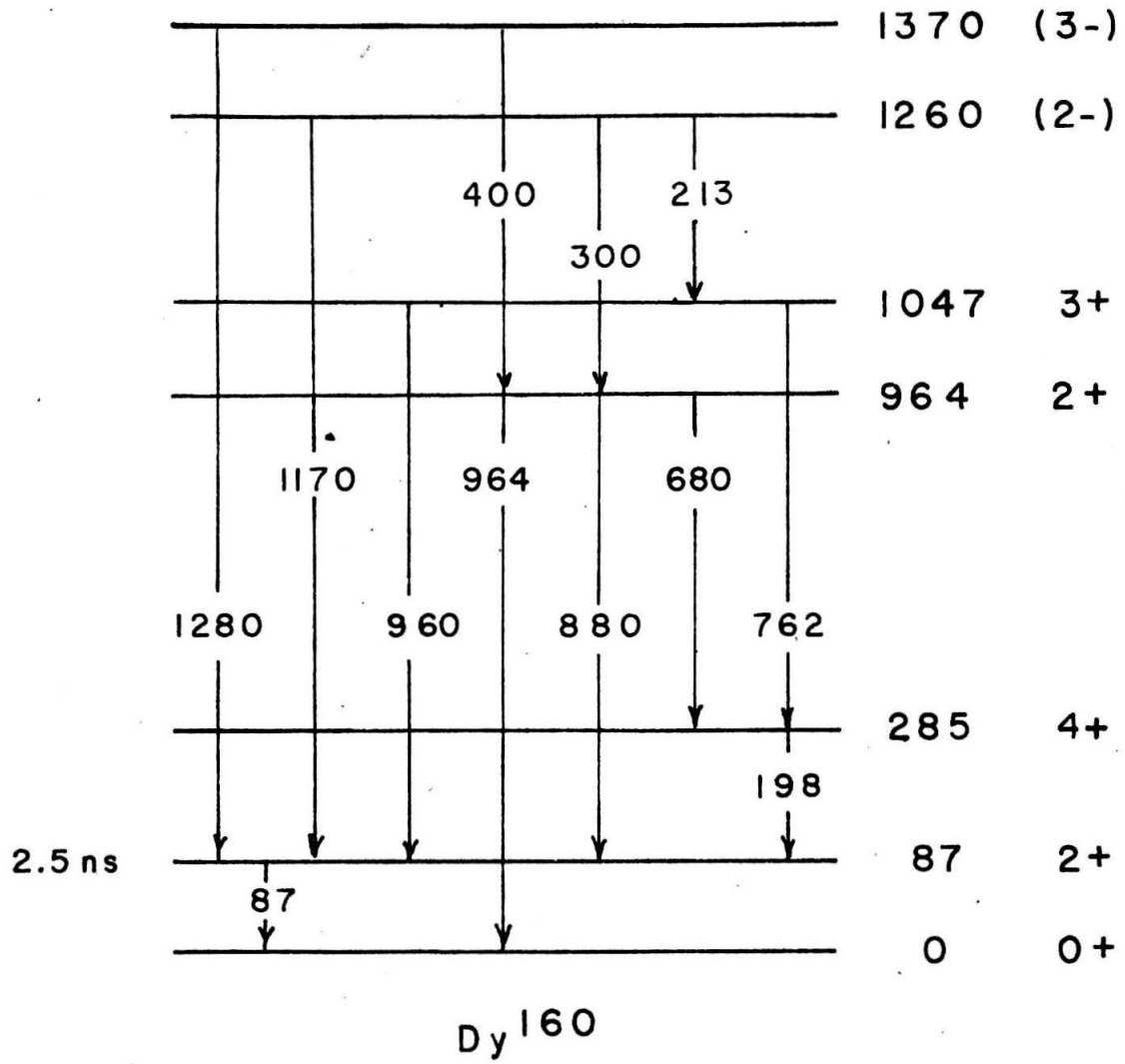

Figure 12. Level structure of Dy^{160}. Energies are in kev and the mean lifetime of the 87 kev level is shown.

g-factor. The result obtained was $g = 0.18 \pm 0.08$. A value of $\beta = 6.2 \pm 0.7$ at $T = 300^{\circ}K$ can be calculated from their results, which compares reasonably well with the value of 6.7 obtained in Appendix I.

The observed attenuation of the angular correlation was attributed by these authors to effects occurring in a time short compared to the nuclear lifetime. Recent work on the decay scheme discussed below suggests that the angular correlation should be unattenuated in liquid sources, while for solid sources the attenuation should be time dependent. Assuming the formulas for liquid sources to hold, and taking the attenuation coefficients $G_2 = G_4 = 0.7$, which can be calculated from their observed angular correlations assuming that the correlations observed in the liquid sources were unattenuated, the result would be $g = 0.24 \pm 0.10$.

Our measurements were done using the composite of the 1,170 - 87 kev and 1,280 - 87 kev cascades. The source used was neutron irradiated Tb_2O_3 dissolved in dilute HCl.

Two measurements of the angular correlatinns of γ-ray cascades in Dy^{160} have been made. S. Ofer[38], using a source of $Tb_2(SO_4)_3$ dissolved in water, obtained for the 1,170 - 87 kev cascade $W(\theta) = 1 + (0.08 \pm 0.02) P_2(\cos\theta) - (0.07 \pm 0.015) P_4(\cos\theta)$, and for the 1,280 - 87 kev cascade, $W(\theta) = 1 + (0.011 \pm 0.02) P_2(\cos\theta) + (0.00 \pm 0.01) P_4(\cos\theta)$. From other measurements, he concluded $G_2 = 0.40 \pm 0.15$, $G_4 = 0.42 \pm 0.04$, for the 87 kev level.

Arns, Sund, and Wiedenbeck[39] have also studied the angular correlations in Dy^{160}. They used a source of Tb_2O_3 dissolved in

dilute HCl. They concluded that the attenuation coefficient for the 87 kev state cannot be measured, but that the results are most consistent with no attenuation for liquid sources. For the 1,170 - 87 kev cascade, they obtained $W(\theta) = 1 + (0.133 \pm 0.041) P_2(\cos\theta) + (0.008 \pm 0.083) P_4(\cos\theta)$, and for the 1,280 - 87 kev cascade, $W(\theta) = 1 + (0.148 \pm 0.065) P_2(\cos\theta) - (0.09 \pm 0.14) P_4(\cos\theta)$.

Our observed angular correlation of the composite 1,170 - 87 kev and 1,280 - 87 kev cascades in the source used for the g-factor measurement was $W(\theta) = 1 + (0.058 \pm 0.005) \cos 2\theta$. After correction for random coincidences and finite solid angle of the counters, this gave $W(\theta) = 1 + (0.091 \pm 0.010) P_2(\cos\theta) + (0.00 \pm 0.02) P_4(\cos\theta)$. A separate measurement of the angular correlation was made for a source of Tb_2O_3 dissolved in dilute HCl, and a source of the same solution with glycerine added to give a viscosity of 10 centipoise. After corrections for random coincidences and finite solid angle, these gave $W(\theta) = 1 + (0.11 \pm 0.01) P_2(\cos\theta) + (0.02 \pm 0.02) P_4(\cos\theta)$ and $W(\theta) = 1 + (0.10 \pm 0.001) P_2(\cos\theta) + (0.00) P_4(\cos\theta)$, respectively. One can conclude that electric quadripole attenuation is not high in these samples. An attenuation coefficient $G_2 = 0.8 \pm 0.12$ can be calculated for the source used in the g-factor measurement.

The g-factor measurement was done at $\theta = 135^\circ$ in a field of 12,000 gauss. The temperature was 340°K. A total of 2×10^5 counts was observed in the 87 kev coincidence peak for each direction of magnetic field. The K x-ray coincidence peak resulting from K-conversion of the 87 kev γ-ray was also observed to assure that there were no significant systematic effects. A value of $R = (4.5 \pm 0.5)\%$

was obtained, which gave a result $G_2\omega\tau = 0.19 \pm 0.03$ radians.

The lifetime of the 87 kev state in Dy^{160} has been measured to be $\tau = (2.6 \pm 0.3) \times 10^{-9}$ sec.[40] The value of β for a temperature of 340°K obtained from Appendix I is $\beta = 6.3$. The attenuation coefficient is taken to be 0.8 ± 0.12, as discussed above. Using these parameters, one can calculate

$$g = \frac{1.36 \pm 0.20}{\beta G_2} = 0.28 \pm 0.08 \quad .$$

4.9 81 kev State of Er^{166}

The g-factor of the 81 kev state in Er^{166} was measured using the 1,370 - 81 kev cascade from the 1,450 kev state. This state was populated by β decay of 27-hour Ho^{166}. The level scheme for this nucleus is shown in Fig. 13.

The angular correlations of the 1,370 - 81 kev cascade in Er^{166} have been measured by two groups. Milton and Fraser[41], using a source of $Ho_2(NO_3)_3$ maintained above its melting point, found $W(\theta) = 1 + (0.137 \pm 0.006) P_2(\cos\theta) + (0.560 \pm 0.019) P_4(\cos\theta)$. Marklund, van Noodjen and Grabowski[42], using an aqueous source of $HoCl_3$ found $W(\theta) = 1 + (0.226 \pm 0.012) P_2(\cos\theta) + (0.783 \pm 0.029) P_4(\cos\theta)$. Both of these correlations are consistent only with a 0 - 2 - 0 decay scheme for which the theoretical correlation is known, although both of these correlations are significantly attenuated from the theoretical value.

Our measurements were made using a dilute hydrochloric acid solution of neutron irradiated Ho_2O_3. Figure 13 shows the

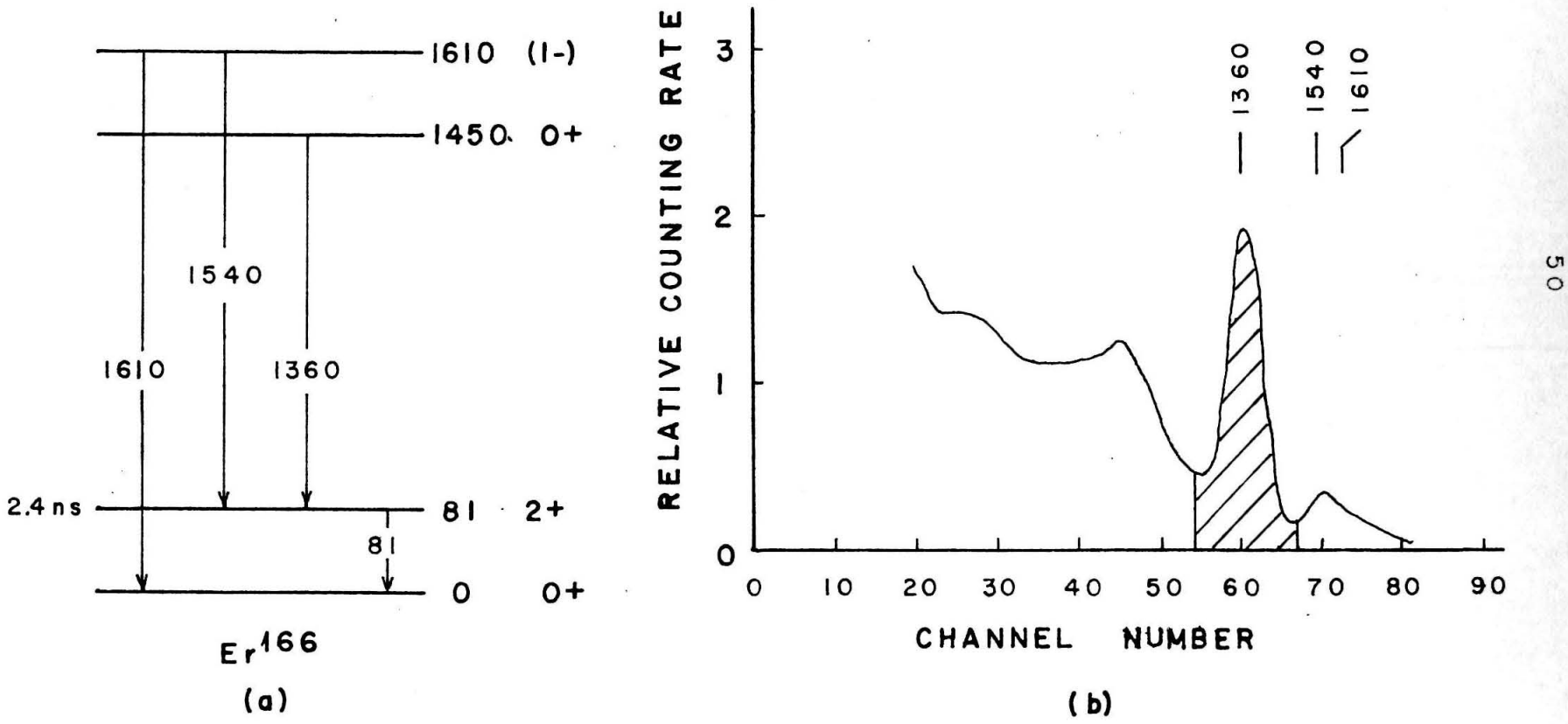

Figure 13. Level structure of Er^{166} and the pulse height spectrum of the Ho^{166} decay. The energies are in kev, and the mean life of the 81 kev level is shown. The cross hatched area shows the setting of the narrow gate.

pulse height spectrum, and the gate set on the 1,370 kev γ-ray. The observed angular correlation, after correction for random coincidences and finite solid angles of the counters was $W(\theta) = 1 + (0.159 \pm 0.03) P_2(\cos\theta) + (0.474 \pm 0.04) P_4(\cos\theta)$. Analysis of the pulse height spectrum of Fig. 13 shows that 25 ± 5% of the γ-rays included in the gate set on the 1,370 kev γ-ray were contributed by the 1,520 kev γ-ray. Using the theoretical coefficients for a (1(D)2(Q)0) transition for this part of the coincidences, and the theoretical coefficients for a (0(Q)2(Q)0) transition for the remainder, the predicted correlation is $W(\theta) = 1 + (0.205 \pm 0.02) P_2(\cos\theta) + (0.36 \pm 0.03) P_4(\cos\theta)$. The attenuation coefficients calculated by comparing these two are $G_2 = 0.78 \pm 0.12$, $G_4 = 0.55 \pm 0.05$. The much larger G_2 value suggests hyperfine attenuation[5]. Since τ_c is expected to be very short, in this case Eqs. (14) and (15) should apply (see Section 2.3).

The g-factor measurements were made at $\theta = 153^\circ$ in a field of 5,000 gauss. The measurements extended over a period of $2\frac{1}{2}$ days, and the angular correlation was measured at the beginning and end. Several measurements of the random coincidence rate were made by inserting a long delay in one counter lead during the course of the experiments. The observed random-to-true coincidence ratio varied from 25% to 5% from beginning to end, and decreased exponentially with the source lifetime. The true coincidence counting rate varied from 60/counts min. to 15 counts/min. during the course of the experiment. In evaluating the results of this experiment, all measurements were corrected for random coincidences but not for finite solid angle. A total of 7,000 counts was observed in the 81 kev

coincidence peak for each direction of magnetic field. The coincidence peak corresponding to the K-conversion x-rays of the 81 kev γ-rays was also observed as a check on systematic effects. The angular correlation, uncorrected for finite solid angle but corrected for random coincidences, was $W(\theta) = 1 + (0.14 \pm 0.02) P_2(\cos\theta) + (0.35 \pm 0.03) P_4(\cos\theta)$. A value of $R = (13.7 \pm 1.3)\%$ was observed. For the 1,350 x-ray cascade, the observed value of R was $(0.3 \pm 2)\%$.

To deduce the rotation from the above measurement, Eq. (14) must be used, since the attenuation is high and the rotation large. Figure 14 shows the dependence of R on $\omega\tau$ using the observed angular correlation coefficients, and the calculated values of G_2 and G_4. The cross-hatched area denotes the observed value of R. The value of $\omega\tau$ found is $\omega\tau = (0.14 \pm 0.02)$ radians.

The lifetime of the 81 kev level of Er^{166} has been measured as $(2.4 \pm 0.28) \times 10^{-9}$ sec.[43] In Appendix I, β is calculated to be 7.7. The resulting value of g, from Eq. (20), is

$$g = 0.31 \pm 0.06 \quad .$$

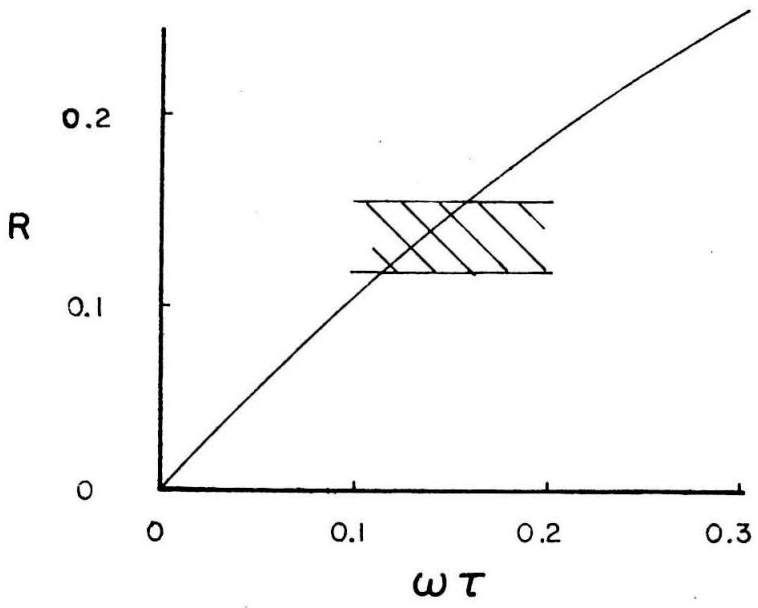

Figure 14. R vs. $\omega\tau$ for Er^{166}. This curve is computed from Eq. (14) using the observed values of the attenuation coefficients and the angular correlation coefficients. The cross hatched area shows the observed value of R.

V. COMPARISON TO THEORY

5.0 Introduction

The magnetic moment of a many-particle nucleus depends very sensitively on the nature of the nuclear force and the details of the nucleon configuration. Since nuclear theory has not progressed to an understanding of these phenomena, the calculation of such magnetic moments is at present impossible.

Because of the inherent difficulty of the problem, most of the progress made in explaining the properties of nuclear states has therefore been through the use of nuclear models. There are presently three of interest in discussing magnetic dipole moments of nuclei. A brief outline of these models as they refer to nuclear magnetic moments is presented below.

The first model of interest is the nuclear shell model[44]. This model visualizes a nucleus consisting of essentially non-interacting particles moving in a spherically symmetric nuclear potential. The properties of such a system are quite analogous to those exhibited by the atomic electron shell. In particular, for instance, each nucleus can be regarded as having an orbital angular momentum, ℓ, and a spin angular momentum, s. For odd-A nuclei, in the simplest picture, the properties of the nuclear state are assumed to be those of the last odd particle, the spins and orbital moments of the other particles being assumed coupled to zero.

Predictions of magnetic moments using this model are easily made for odd-A nuclei. Using the free nucleon values for spin and

orbital g-factors, one obtains[44] for a nucleus with odd Z,

$$\mu = (2.79 + I - \tfrac{1}{2})\,\mu_n \qquad \text{for } I = \ell + \tfrac{1}{2}$$
$$\mu = \frac{I}{I+1}\,(-2.79 + I + \tfrac{3}{2})\,\mu_n \qquad \text{for } I = \ell - \tfrac{1}{2} \tag{21}$$

while for an odd-N nucleus,

$$\mu = -1.91\,\mu_n \qquad \text{for } I = \ell + \tfrac{1}{2}$$
$$\mu = \frac{I}{I+1}\,1.91\,\mu_n \qquad \text{for } I = \ell - \tfrac{1}{2} \tag{22}$$

These formulas give the so-called Schmidt limits for the magnetic moments, which although confirmed in a few cases by experiment, are generally in error by as much as 50%. However, in virtually all cases where they are applicable, the Schmidt limits do indeed furnish an upper or lower limit for $I = \ell + \frac{1}{2}$ and $I = \ell - \frac{1}{2}$, respectively. Since several factors such as configuration admixtures and residual interparticle forces are ignored in this calculation, it is not surprising that many experimental results are in disagreement with it.

More recently, the collective model of Bohr and Mottleson[45] has had some success in explaining the properties of nuclei in certain regions of the periodic table. The basic concept of this model is that the nucleus has an ellipsoidal rather than a spherical shape. This gives rise to nuclear energy levels coming from a collective rotation of the nucleus around an axis perpendicular to its axis of symmetry. The assumption is made that the rotation of the nucleus does not affect its intrinsic configuration. This simple model has had striking

success in explaining the properties of low-lying nuclear states for heavy nuclei lying between closed nuclear shells in the periodic table. (See for instance Alder, et al[21] for a summary of experimental results.)

The rotational motion now contributes to the magnetic moment of the nucleus. Using the usual terminology for this model, where I is the total nuclear spin, K the quantum number associated with the intrinsic angular momentum of the nucleus (and also the spin of the state upon which a rotational band is based), and g_K and g_R the g-factors associated with the intrinsic and rotational motions respectively, the magnetic dipole moment of a nucleus for $K \neq \frac{1}{2}$ can be written

$$\mu = \left[g_R I + (g_K - g_R) \frac{K^2}{I+1} \right] \mu_n . \qquad (23)$$

(The additional complexity associated with $K = \frac{1}{2}$ is discussed in the section on Tm^{169} below.) It is a consequence of the model that g_K and g_R in Eq. (23) should be constant in any rotational band. It can be seen that if this is indeed the case, measurement of two magnetic moments in one rotational band allows independent calculation of g_K and g_R, when $K \neq 0, \frac{1}{2}$, while in a band with $K = 0$, measurement of only one g-factor determines g_R.

Theoretical predictions for the value of g_R depend upon a knowledge of the details of the nuclear flow. The simplest models of rigid rotation or perfect hydrodynamic flow, where the nuclear matter moves as a uniformly charged fluid, give $g_R = Z/A$. One would expect, however, that g_R does not vary rapidly from nucleus to

nucleus in a given region of the periodic table.

The value of g_K in this model can be predicted only by making definite assumptions about the intrinsic nuclear structure. The unified nuclear model does this by assuming that the general concepts of the shell model apply to the ellipsoidal nuclear potential assumed in the collective model above. Nilsson[18], for instance, has calculated the ordering and wave functions for the single particle states in an ellipsoidal harmonic oscillator potential with added $\ell \cdot s$ coupling as a function of a deformation parameter, δ. By making the assumption that the intrinsic nuclear properties of odd-A nuclei stem from the motion of the last odd particle, he is able to predict ground state spins, nuclear moments, and other nuclear properties. Formulas for g_K are given in this work as a function of the tabulated wave functions.

Mottleson and Nilsson have applied this model to the properties of many odd-A nuclei in a recent paper[46] with marked success. Figures 16 and 17 of this reference show theoretical and experimental magnetic moments for nuclear ground states, calculated using $g_R = Z/A$. There is a consistent disagreement to be seen of the order of $0.6\,\mu_n$ or less in virtually all moments plotted. This rather consistent small deviation may possibly arise from the effects of residual interparticle forces not considered in the chosen potential. It should be noted that configuration mixing is much more accurately considered in this model than in the simple nuclear shell model.

In the several subsections below, each nucleus is studied and

treated separately, and the interpretation of the result is discussed in terms of the applicable model theory.

5.1 As^{75}

The As^{75} nucleus is one in which one might hope, by using measured values of magnetic moments and other nuclear parameters, to justify the use of one or another of the nuclear models. The magnetic moments can be calculated from the simple shell model formulas of Eqs. (21) and (22). The results for the ground state and the 280 kev state are $3.75\,\mu_n$ and $0.87\,\mu_n$, respectively. These values can be compared to the measured values of $1.43\,\mu_n$ and $(0.42 \pm 0.13)\,\mu_n$, respectively. Especially for the ground state moment this agreement is rather poor.

Manning and Rogers[47] have shown that several properties of the low-lying states of As^{75} can be understood on the basis of the unified model. The ground state and the 280 kev state are assigned to Nilsson orbits 16 and 15, respectively. Figure 15 shows the theoretical magnetic moments of the two states plotted as a function of δ, the distortion parameter. $g_R = Z/A$ has been used in the calculation. The value $\delta = 0.2$ shown on the graphs is that predicted from the measured ground state quadripole moment. The measured magnetic moments can be seen to be in qualitative agreement with those predicted on the Nilsson picture, and can thus be said to be consistent with the proposed model explanation. Since these states are both single-particle states, a separate calculation of g_K and g_R is not possible.

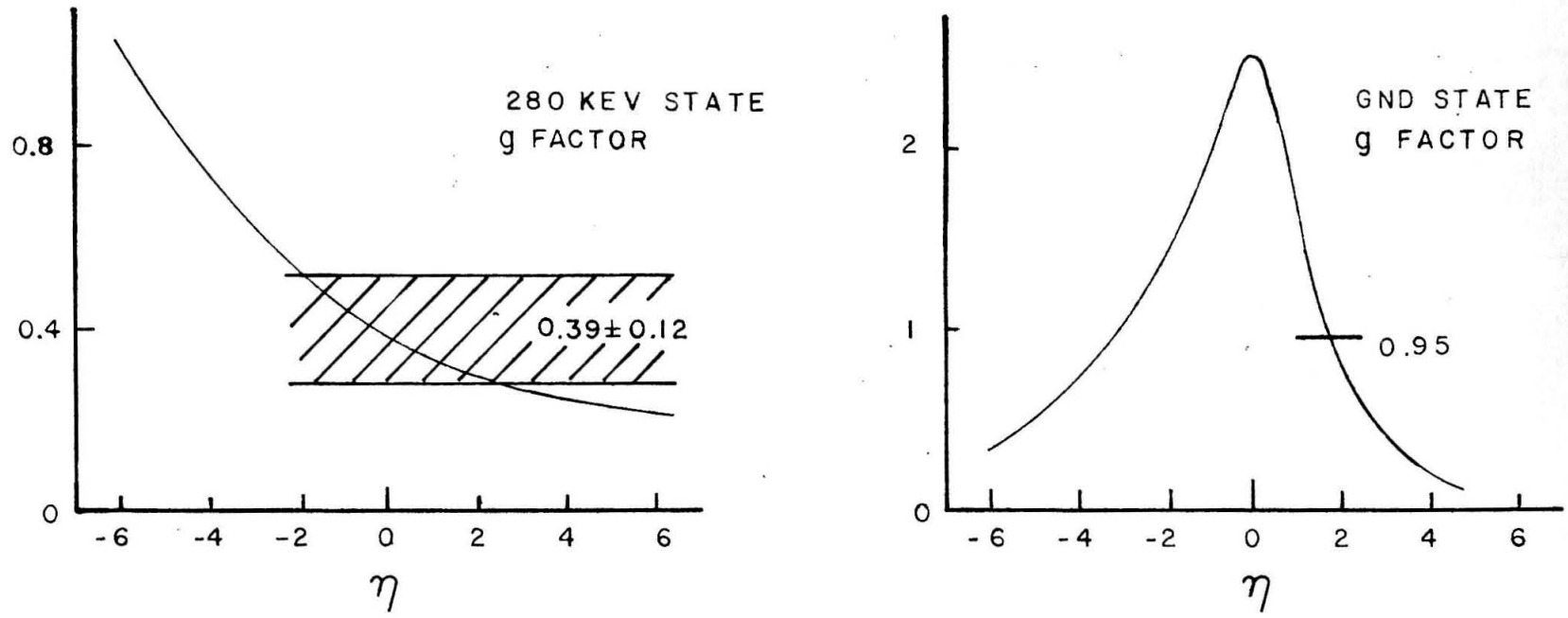

Figure 15. Magnetic moments of the ground state and 280 kev state of As^{75} according to the Nilsson model. The ground state is assigned to Nilsson orbital 16, and the 280 kev state to orbital 15. The cross hatched area shows the experimentally determined values of g.

5.2 Pm^{147}

A somewhat different outlook must be taken for Pm^{147}. Very little is known about this nucleus. The spin and magnetic moment of the ground state have not been measured, and the spin of the 91 kev state is not known. Shell model considerations have suggested spins of 5/2+ and 7/2+ for the ground state and the first excited state with an uncertain order. It is possible to differentiate between these two possibilities on the basis of this measurement.

The shell model prediction of the g-factor is $g = 0.49$ for a 7/2+ state, and $g = 1.92$ for a 5/2+ state in an odd-Z nucleus from Eq. (21). Our measurement, $g = 0.9 \pm 0.2$, would seem to rule out the 7/2+ spin for the 91 kev state.

It must be said that while this measurement illustrates the possibility of g-factor measurements playing a role in the assignment of nuclear spins, a real understanding of the structure of this nucleus awaits future clarification of the level scheme.

5.3 Tm^{169}

Tm^{169} is a highly deformed nucleus, and the unified model has had considerable success in predicting the properties of its low-lying levels. It is therefore of considerable interest to attempt a detailed comparison of the magnetic moments with the model predictions.

The properties of the low-lying states of this nucleus were extensively studied by Hatch, Boehm, and Marmier[48]. Their re-

sults, as summarized by Mottleson and Nilsson[46], show the 5/2+, 118 kev state as the second rotational state based on the 1/2+ ground state. δ is found to be 0.28 and the decoupling parameter, a, is -0.77. The ground state is identified with the $(411\frac{1}{2})$ orbital.

Since the ground state of this rotational band has $I = 1/2$, a slightly more complicated formula for the moment must be used. From Reference 18 the magnetic moment for the case $K = 1/2$ is

$$\mu = \left[\frac{I}{4(I+1)} (g_K - g_R) \left[1 - (2I+1)(-1)^{I-\frac{1}{2}} b_o \right] + I g_R \right] \mu_n . \quad (23)$$

The constant b_o, related to the decoupling parameter a, must now also be determined from the results along with g_K and g_R. Three experimental quantities instead of the previous two must therefore be used to determine these constants. In principle, the reduced M1 transition probability between two of the rotational states may be used with the ground and excited state moments for this purpose, but the results are not sufficiently accurate to be of interest. Bernstein and de Boer[49] have used two such M1 transition probabilities determined from Coulomb excitation data together with the ground state moment to obtain $g_R = 0.23 \pm 0.12$, $g_K = -1.76 \pm 0.21$, $b_o = 0.0 \pm 0.12$. Using these values, one can calculate the expected moment of the 5/2+ state as $\mu = 0.45 \pm 0.50$ in crude agreement with our value of $\mu = 1.0 \pm 0.3$.

Using the Nilsson wave functions, the variation of the g-factor for the 5/2+ state with deformation parameter η has been calculated. The results are shown in Fig. 16, where the solid line is for $g_R = 0.4$

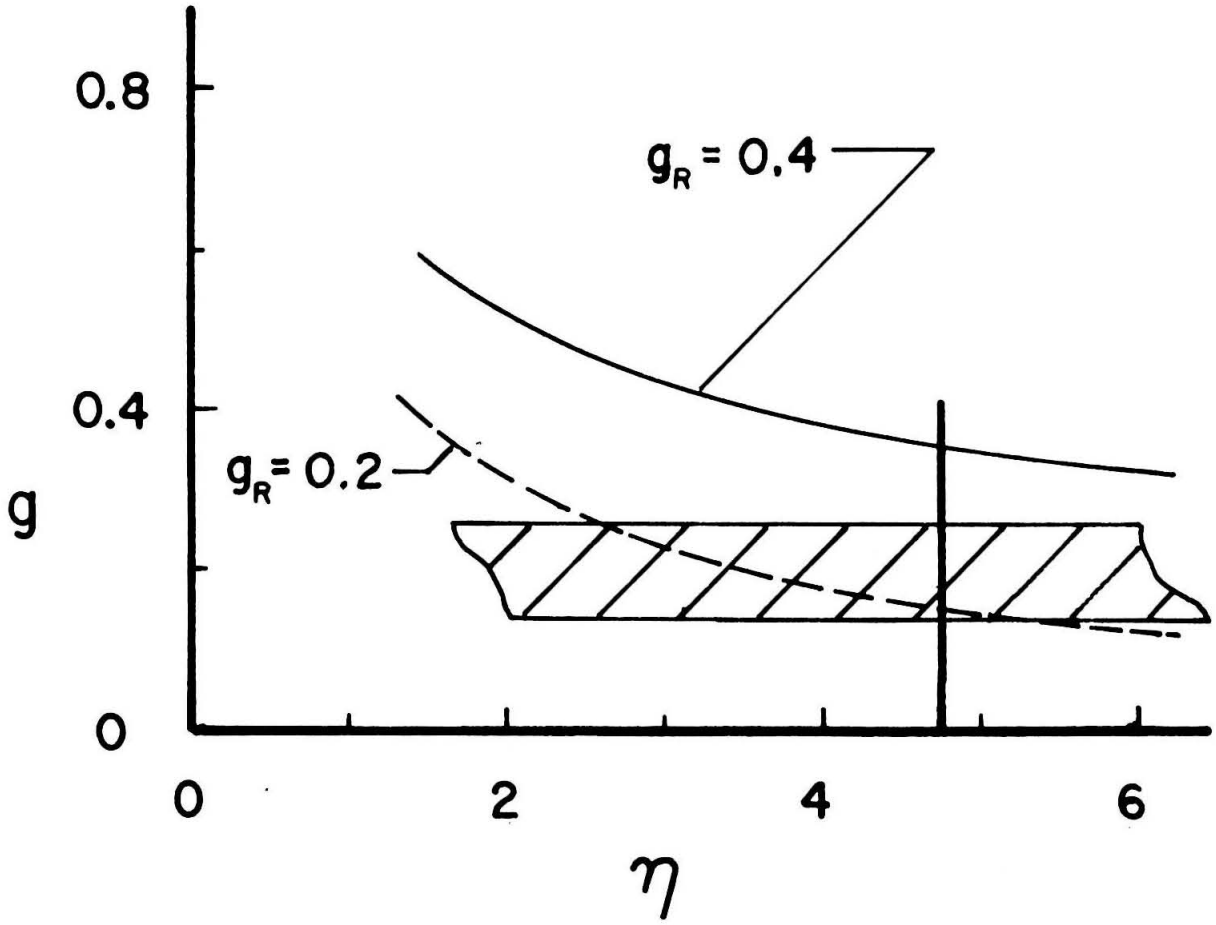

Figure 16. The calculated g-factor for the 118 kev state of Tm^{169} according to the Nilsson model. The cross hatched area shows the experimental result. The assumed deformation ($\eta = 4.8$) is indicated.

and the dotted curve is for $g_R = 0.2$. (The measured rather than the calculated values of the decoupling parameter, a , were used for these curves.) The assumed deformation is indicated. It can be seen that this result is in agreement with the theory for $g_R = 0.2$.

Interpretation of these results is rather difficult. The agreement between our measurement and the Nilsson prediction is not shared by the values of Bernstein and de Boer, since for the observed deformation the calculated g_K is -2.4. However, our results are in agreement with those of Bernstein and de Boer within the quoted errors. The situation could perhaps be clarified by the measurement of the magnetic moments for the 3/2+ level and the 7/2+ level. Both of these experiments appear feasible, and the results could provide a very interesting check on the theory.

5.4 Lu^{175}

Marmier and Boehm[50] have studied the level structure of Lu^{175}. Their results, as quoted in Mottelson and Nilsson[46] show reasonable agreement with the predictions of the unified nuclear model, and it is of interest to see if the predictions of the model for the g-factor can be verified as well.

The 9/2+, 114 kev level in Lu^{175} is identified as the first rotational state based on the 7/2+ ground state. The ground state is identified as the (404 7/2) orbital with $\mu = 0.28$. The measured value of the ground state moment is $\mu = (2.0 \pm 0.2)\mu_n$.[51] Using experimental values of the reduced transition probability and the ground state moment, Berstein and de Boer obtained $g_R = 0.30 \pm$

0.06, $g_K = 0.65 \pm 0.06$.

Using the ground state moment quoted above, and the excited state moment of $\mu = (2.2 \pm 0.9)\mu_n$, the values of g_K and g_R are found to be $g_K = 0.51 \pm 0.20$, $g_R = 0.8 \pm 0.7$. The g_K predicted from the unified model for the chosen deformation is $g_K = 0.41$. This value is somewhat in disagreement with the value obtained by Bernstein and de Boer, but is included within the error of our rather less accurate result.

5.5 Hf^{177}

The level structure of Hf^{177} has been studied by Hatch, Boehm, Marmier, and Du Mond[52]. Their results are summarized in Reference 46. They interpret the 113 kev 9/2- level as the first rotational state based on the 7/2- ground state, which is assigned as the (514 7/2) orbital with a deformation parameter $\delta = 0.27$. The measured ground state magnetic moment is $\mu = (0.61 \pm 0.03)\mu_n$.[53] Using experimental values of the reduced M1 transition probabilities, Bernstein and de Boer found $g_R = 0.215 \pm 0.014$, $g_K = 0.162 \pm 0.010$.

The value of the magnetic moment for the 9/2- state resulting from our experiment is $\mu = (0.90 \pm 0.27)\mu_n$. Combined with the ground state moment, this yields $g_R = 0.24 \pm 0.16$, $g_K = 0.15 \pm 0.04$. The theoretical prediction using the Nilsson wave functions is $g_K = 0.41$. The experimental values of g_K are in agreement, and both show marked disagreement with the predictions of the model.

5.6 Even-Even Nuclei

As is pointed out in the first part of this section, measurement

of the g-values of the first rotational state of an even-even nucleus constitutes a direct measurement of g_R. Three such g-factors have been measured in this work with a sufficient accuracy to be of practical interest; Sm^{152}, Dy^{160}, and Er^{166}. The fourth measurement, Gd^{154}, is interesting in that it serves to confirm many of the assumptions made in deriving the paramagnetic correction factor as well as pointing out the dangers inherent in these measurements where the assumptions made are not fulfilled.

Table 2 is a summary of the existing measurements on g-factors of the first rotational states of even-even nuclei. These results are obtained from experiments similar to these, and experiments utilizing angular distribution rotation measurements following Coulomb excitation. (The corrections to the results of Goldring and Scharenberg, and Sugimoto for the case of Sm^{152} are discussed in Section 4.6.) The measurements quoted seem to show a trend in g_R from values of about $\frac{1}{2}$ Z/A at the lowest A values, to values approximating Z/A in the case of high A. Unfortunately, there are not enough results of sufficient accuracy to warrant drawing detailed conclusions about the variation of g_R with A.

The values of g_R for many odd-A nuclei have been calculated by Bernstein and de Boer[49] from Coulomb excitation measurements of reduced M1 transition probabilities and the known ground state moments. The results are shown in Fig. 17. The values of g_R for even-even nuclei quoted in Table 2 have been included for comparison. The trend of the g_R values with A appears very similar for odd-A and even-even nuclei, the predominant difference being the low values of g_R for even-even nuclei in the region of $A = 150^{\circ}$.

TABLE 2

g_R for even-even nuclei

Nucleus	Z/A	Experimental Values	Ref.
$_{60}Nd^{150}$	0.40	0.22±0.04	(a)
$_{62}Sm^{152}$	0.41	0.30±0.06*	(a)
		0.28±0.07	(b)
$_{66}Dy^{160}$	0.41	0.18±0.08	(c)
		0.28±0.07	(b)
$_{68}Er^{166}$	0.41	0.31±0.06	(b)
$_{74}W^{184}$	0.40	0.38±0.05	(d)

(a) Goldring and Scharenberg [29]

(b) present work

(c) Debrunner et al [37]

(d) Bodenstedt et al [60]

* Corrected for effects of paramagnetism according to Appendix 1.

Summary of experimental results for the rotational g-factor g_R of even-even nuclei.

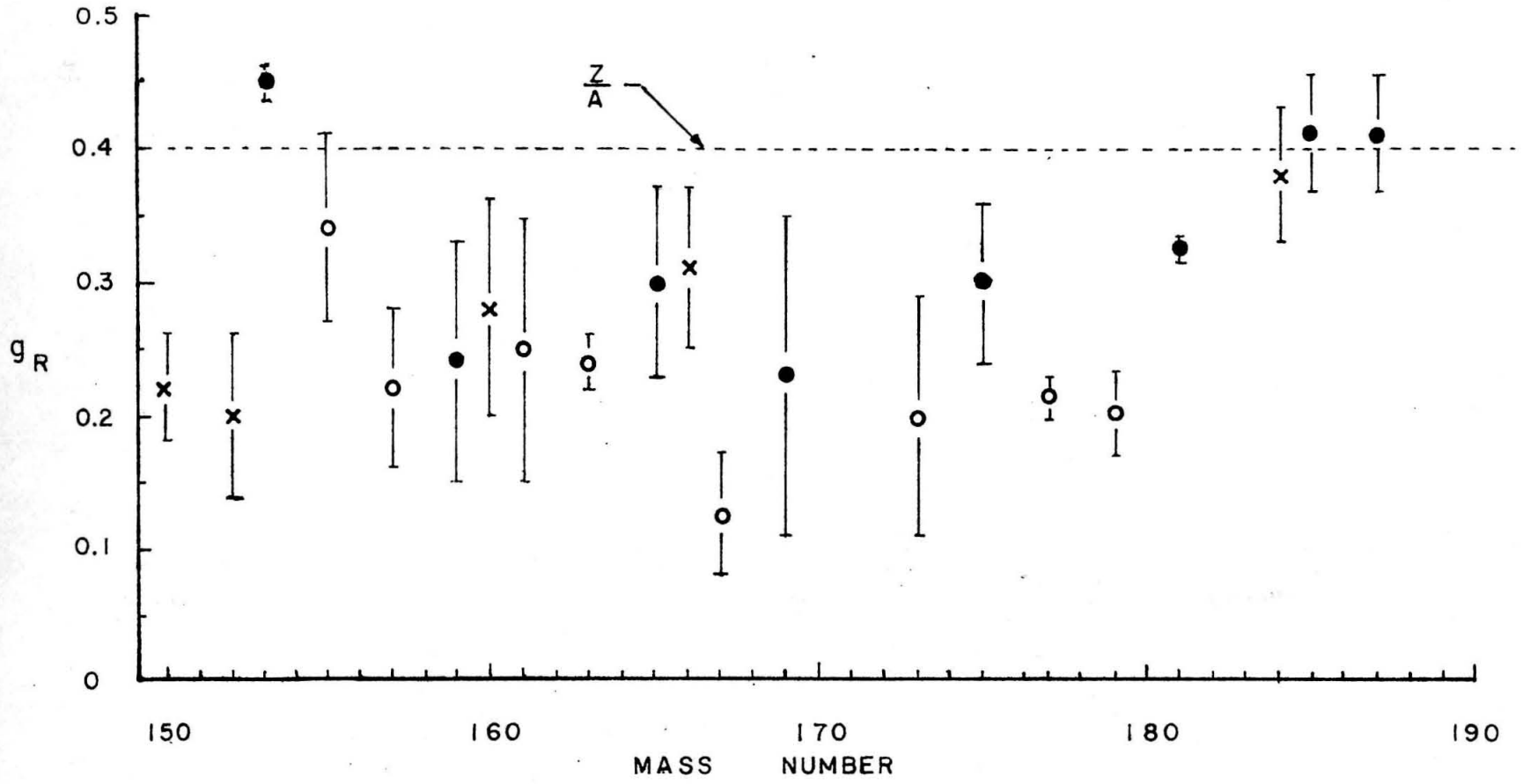

Figure 17. Experimental values of g_R. The solid and open circles are for odd-Z and odd-N nuclei respectively. The values are taken from Ref. 49. The crosses show values for even-even nuclei taken from Table 2.

VI. CONCLUDING REMARKS

6.0 Discussion

We have seen that in these experiments, the directly measured quantity is the rotation of an angular correlation for some γ-ray cascade in an applied magnetic field. The rotations have been interpreted in terms of g-factors, using the formulas developed in Section 2.

In deriving these formulas, certain assumptions have been made concerning the effect of electron paramagnetism, as expressed in the formulas by the parameter β, and concerning the nature of any attenuation of the angular correlation, as expressed by the parameters g_K. The validity of the interpretation of the rotation in terms of a g-factor depends on the validity of these assumptions. It is therefore well to summarize them briefly.

In the calculation of the paramagnetic correction factor β for the 3+ rare earth ions, it was assumed that:

1. The nuclei interact with the time average of the z-component of the field due to the paramagnetic electrons. This requires that the time, τ_c, in which the electronic magnetic field changes its orientation, be very short compared to the nuclear lifetime, as well as that the nuclear precession frequency in the electron field be small compared to $1/\tau_c$.*

2. The electronic configuration of the ion containing the nucleus must be that of the 3+ daughter ion during the intermediate state of the nucleus. This requires in many cases a very rapid reorientation of the electronic configuration.

If there is an attenuation of the angular correlation, then it is also assumed that:

3. Any attenuation of the angular correlation must be unaffected by application of an external magnetic field, and must, further, result from an interaction with a field whose characteristic time, τ_c, for remaining constant in direction is very small compared to the nuclear lifetime.

Attenuation caused by interaction of the nuclear electric quadripole moment with the fluctuating electric fields in a liquid, and certain types of attenuation caused by interaction of the nuclear magnetic dipole moment with a paramagnetic electron shell in a liquid, fulfill the above requirements. Attenuations in solids may not.

In the derivations of Appendix I and Section 2, the justification of some of these assumptions is discussed, and the paucity of direct evidence as to their validity (especially assumption 2) is mentioned.

Our experiments, however, do furnish considerable indirect evidence that these assumptions are justified, some of which may be briefly summarized.

First, several of the g-factors observed have been measured by other methods, using for instance different methods of populating the intermediate state (Sm^{152}), or a source in a different form (Tb^{160} and Sm^{152}). The agreement found is satisfactorily within the errors in these cases. In two cases, Hf^{177} and Lu^{175}, derived values of g_K and g_R for odd-A rotational nuclei can be compared to similar results obtained from an interpretation of Coulomb excitation data.

The results are in agreement. The case of Gd^{154}, in which paramagnetic attenuation was found to be severe, can be explained as an expectable breakdown of assumptions 1 and 3, but requires that assumption 2 be fulfilled. Finally, there is a direct measurement of the paramagnetic correction factor for a solid Tb^{160} source obtaining results in agreement with those predicted. One can conclude from this that the evidence for the validity of this method of measuring g-factors, provided that care is taken to consider special cases, is very good.

The separate discussions of the interpretation of each measurement demonstrated some of the different possible uses a g-factor measurement may serve. In the case of As^{75}, the measurement served as a check on the explanation of the nucleus in terms of the unified model. In Pm^{147} it was possible to make a tentative assignment of a spin on the basis of shell model considerations. For the odd-A nuclei known to be collective in nature, the measurement served to predict g_R and g_K, the latter of which can be predicted from the Nilsson model. In the case of the even-even collective nuclei, our measurements served as a direct evaluation of g_R, a parameter of considerable interest in the theory of the collective model.

The results of the measurements on the odd-A collective nuclei suggest that there is some discrepancy between the measured values of g_K and those predicted by the Nilsson model. These measurements, on the other hand, are not a sensitive measurement of g_R.

Our measurements on even-even collective nuclei in the rare earth region indicate that there is considerable deviation of the rotational g-factor, g_R, from the value $g_R = Z/A$. This deviation seems to vary with atomic number as well. More work in this area would probably be of interest to the theory of the unified and collective models.

APPENDIX I

Paramagnetic Correction Factor

This appendix discusses the calculation of the effect of electron paramagnetism on angular correlations in an applied magnetic field. The effect is calculated for the rare earth 3+ ions, which are assumed to be in a liquid solution. It is assumed from evidence discussed in Section 2.4 that the nucleus interacts with the time average of the z-component (along the direction of the applied field) of the electronic magnetic field. If this assumption is correct, the effective magnetic field, H_{eff}, at the nucleus when an external magnetic field, H, is applied, is in the direction of H and can be written

$$H_{eff} = \beta H . \qquad (1A)$$

The calculation of β is the subject of this appendix.

In order to calculate β, the electronic configuration of the ion during the intermediate state of the nucleus must be known. Because of the previous nuclear transitions, this may be difficult to ascertain. A typical case we encounter is that of a β decay followed by a γ-ray cascade. At the beginning of this event, the ion is assumed to be in the 3+ ionization state of the parent element. Sometime during or after the event, the ion reaches the stable 3+ configuration of the daughter element. If the time for reorganization of the electronic shell is very short or very long compared to the nuclear lifetime, the effect can be calculated.

Some relevant times for such reorientations to occur in a liquid can be inferred from various sources. The correlation time,

τ_c for water molecules in water is known to be $\sim 10^{-12}$ sec.[5] This number is related to the collision time in the liquid and is expected to be similar for ions in solution[5]. Goldring and Scharenberg[29] state that a paramagnetic relaxation time of less than 10^{-12} sec. is required to explain their observed angular distribution results from Nd^{3+} and Sm^{3+} ions in solution. This time is essentially the time in which the electronic angular momentum changes its orientation, and is again closely related to the collision time. Collisions will play a strong role in de-exciting any excitatinns of the outer electrons, and one therefore would expect that this type of excitation would be removed in 10^{-12} sec. or less for paramagnetic ions in solution.

In the case of a β decay, it is also necessary for the ion to pick up an extra electron, while for a K-capture event, it may need to acquire as many as five or six electrons to compensate for the loss of Auger electrons in the resulting x-ray cascade. The time necessary for picking up an electron is difficult to estimate, and there is no direct experimental evidence available. One might again suppose that a relevant time would be the collision time.

On the basis of the above discussions, it is reasonable to assume that the electronic structure is that of the 3+ ion of the daughter element during the intermediate state, and therefore, the calculation is done on this basis. The specific calculation of the β-values with the above assumptions has been discussed by Goldring and Scharenberg[29] for some isotopes, by Manning and Rogers[47], and by Kanamori and Sugimoto[34]. The results obtained are similar, with the

exception that Kanamori and Sugimoto have pointed out that for the case of Eu^{3+}, Sm^{3+}, and Pm^{3+} a more accurate treatment is required than that given by Manning and Rogers. The derivation of the formulas of Kanamori and Sugimoto (which contain some numerical errors) and Manning and Rogers is given below.

The electronic structure of rare earth 3+ ions is discussed by Eliot and Stevens[54] and by van Vleck[55]. The electronic configuration of the rare earths is of the form $(4f)^n$ where n varies from 1 to 14. L-S coupling is appropriate, and the electronic states can be characterized by L, S and J, in the usual way. The ground electronic state is determined by Hund's rule. Energy splittings of the ground state J due to the crystalline fields are small compared to KT at room temperature, and thus can be ignored. The first excited electronic state, characterized by L, S, J', falls from $400^{\circ}K$ to $10,000^{\circ}K$ above the ground state, and is thus not significantly populated at room temperature.

The energy of interaction between the electronic structure and an applied magnetic field is of the form[55]:

$$H_1 = \mu_o \vec{H} \cdot (\vec{L} + 2\vec{S}) \ . \qquad (2A)$$

For L-S coupling states, this gives rise to a set of energy levels which can be specified (to first order) by J and M, the total angular momentum and its projection on the axis of the field. The energy is

$$E(JM) = \mu_o g_L H M \ , \qquad (3A)$$

where g_L is the Lande g-factor.

The energy of interaction of the nucleus with the atomic electron shell can be written as[54]:

$$H_2 = \sum_i 2\mu_o\mu_n g_n \left\langle \frac{1}{r_i^3} \right\rangle \left[\ell_i - s_i + 3 r_i \frac{(r_i - s_i)}{r_i^2} \right] \cdot \frac{I}{I} , \qquad (4A)$$

where the sum is over all unpaired electrons, and ℓ_i is the orbital angular momentum, s_i the spin angular momentum, and r_i the coordinate of the i^{th} electron. The contribution from s electrons has been ignored. Eliot and Stevens define an operator N such that

$$H_2 = 2\mu_o\mu_n g_n \left\langle \frac{1}{r^3} \right\rangle N \cdot I . \qquad (5A)$$

The nucleus also interacts directly with the applied external field. The energy of this is

$$H_3 = \mu_n g_n H \cdot I . \qquad (6A)$$

If the eigenstates of H_1 are assumed of the form $|JM\rangle$, and states of only one J are populated, then, since the z-component only is of interest, the time average of H_2 can be written

$$H_2 = 2\mu_o\mu_n g_n \left\langle \frac{1}{r^3} \right\rangle I_z \sum_M \frac{\langle JM|N_z|JM\rangle e^{-E(JM)/KT}}{\sum_M e^{-E(JM)/KT}} . \qquad (7A)$$

Eliot and Stevens show that the quantity $\langle JM|N_z|JM\rangle$ can be written as

$$\langle JM|N_z|JM\rangle = \langle J\|N\|J\rangle \langle JM|J_z|JM\rangle ,$$

where the "reduced matrix elements" $\langle J\|N\|J\rangle$ are independent of M and are tabulated for each element. Upon expanding the Boltzman

factor, H_2 can be written as

$$H_2 = 2\,\mu_o\,\mu_n\,g_n\left(\frac{I}{r^3}\right) I_z \langle J\|N\|J\rangle \quad \frac{\sum_{-J}^{J} M - \frac{\mu_o g_L H M^2}{KT}}{2J+1} \,. \qquad (8A)$$

which becomes

$$H_2 = 2\mu_n g_n \left(\frac{I}{r^3}\right) \frac{\langle J\|N\|J\rangle}{g_L} \frac{\mu_o^2 g_L^2 J(J+1)}{3KT} H I_z \,. \qquad (9A)$$

Now $\beta - 1$ is just the ratio of this to H_3, or

$$\beta - 1 = \frac{H_2}{H_3} = 2\left(\frac{I}{r^3}\right) \frac{\langle J\|N\|J\rangle}{g_L} \frac{\mu_o^2 g_L^2 J(J+1)}{3KT} \,. \qquad (10A)$$

Van Vleck's definition[55] of μ_{eff} under the assumptions made (multiplet splittings wide compared to KT) is

$$\mu_{eff}^2 = g_L^2 (J)(J+1) \,. \qquad (11A)$$

Also, with this assumption, Eliot and Stevens give

$$2\left(\frac{I}{r^3}\right) \frac{\langle J\|N\|J\rangle}{g_L} = \left(\frac{A}{g_{\|} g_n}\right)\left(\frac{1}{\mu_n \mu_o}\right) \,. \qquad (12A)$$

In their notation, $g_L = \langle J\|\wedge\|J\rangle$. All of this derivation depends on the separation of the first excited electronic level being far above the ground level.

For Sm^{3+}, Eu^{3+}, and Pm^{3+}, this approximation is not good, as pointed out by Kanamori and Sugimoto[34]. For these cases, the mixing of the first excited state into the ground state by means of the magnetic field (the second order Zeeman effect) is significant at room

temperature. The result of this can be seen in the susceptibility measurements, for instance. M is still an eigenvalue of H_1, and the eigenstates of H_1 can be written

$$|\propto M\rangle = |JM\rangle + \sum_{J' \neq J} \frac{\langle JM|H_2|J'M\rangle}{E_J - E_{J'}} |J'M\rangle \quad . \qquad (13A)$$

In practice, only $J' = J \pm 1$ contributes. The time average of H_2 then becomes

$$H_2 = 2\mu_o \mu_n g_n \left(\frac{I}{r^3}\right) I_z \cdot$$

$$\frac{\sum_M \left[\langle JM|N_z|JM\rangle + \sum_{J'} \frac{\langle JM|N_z|J'M\rangle\langle J'M|H_2|JM\rangle}{E_J - E_{J'}}\right] e^{-\frac{E(\propto M)}{KT}}}{\sum_M e^{-\frac{E(\propto M)}{KT}}} \qquad (14A)$$

or, upon expanding the Boltzman factor and summing,

$$H_2 = 2\mu_n g_n \left(\frac{I}{r^3}\right) \frac{\langle J||N||J\rangle}{g_L} \frac{\mu_o^2 g_L^2 J(J+1)}{3KT} H \cdot I_z$$

$$+ \frac{1}{2J+1} \sum_M \sum_{J'} \frac{\langle JM|N_z|J'M\rangle\langle J'M|H_2|JM\rangle}{E_J - E_{J'}} \cdot I_z \, , \qquad (15A)$$

and

$$\beta - 1 = \frac{H_2}{H_3} = 2\left(\frac{I}{r^3}\right) \frac{\langle J||N||J\rangle}{g_L} \frac{\mu_o g_L (J)(J+1)}{} +$$

$$+ \frac{1}{2J+1} \frac{1}{\mu_o g_L H} \sum_M \sum_{J'} \frac{\langle JM|N_z|J'M\rangle\langle J'M|H_2|JM\rangle}{E_J - E_{J'}} \, . \qquad (16A)$$

The factors $\langle J||N||J\rangle$, and $g_L = \langle J||\Lambda||J\rangle$ are given by Eliot and Stevens, as well as the matrix elements $\langle J, M|N_z|J\pm1, M\rangle$ and $\langle JM|L_z + 2S_z|J\pm1, M\rangle$. The values of $E_J - E_{J'}$ are also tabulated. Values of $(\frac{T}{3})$ accurate to about 5% are given by Baker and Bleaney[56]. Table A-1 lists the relevant parameters for each ion, and shows β-1 from Eq. (10A) in column 6, and β-1 for Pm^{3+} and Sm^{3+} from Eq. (16A) in column 7. The effect is small except for Sm^{3+}.

It can be mentioned that for the case where Eq. (10A) applies, namely, no admixtures of other J states, the ratio $A/(g_{\|}g_n)$ is independent of the coupling model used for the electrons. Crystalline field splittings and breakdown of L-S coupling, for instance, do not affect this ratio. Since the value of μ^2_{eff} can be gotten from susceptibilities[55], and the value of $A/(g_{\|}g_n)$ can be measured experimentally by paramagnetic resonance, the value of β-1 can be checked against that derived from experimental quantities. The result, as shown in Manning and Rogers[47] is given in column 8 of Table A-1. The agreement is in general good, except in the cases mentioned.

The calculation of β for Gd^{3+} is not applicable to the experiments, since it is believed that the assumption of thermal equilibrium made for the electron shell is not valid in this case (see Section 2.4).

TABLE A1

PARAMAGNETIC CORRECTION FACTOR

1	2	3	4	5	6	7	8
ion	$\frac{\langle J \Vert N \Vert J \rangle}{g_L}$	μ_{eff}	$(\frac{1}{r^3})$ (A^{0-3})	$\frac{A}{g_{\Vert}\, g_n}$ $(cm^{-1} \times 10^{-2})$	β-1	β-1 corrected	β-1 exp.
La	-	0	-	-	0	0	-
Ce	1.60	2.54	32.5	2.79	0.4		0.5
Pr	1.65	3.58	37	3.13	1.0		1.2
Nd	1.81	3.62	42	3.76	1.3		1.5
Pm	2.26	2.68	47		1.0	0.92	
Sm	5.42	0.84	51	4.18	0.9	0.15	0.3
Eu		0	57				
Gd	0	7.84	62		0	0	-
Tb	0.36	9.7	68	1.18	3.0		3.2
Dy	0.53	10.6	74		5.8		
Ho	0.61	10.6	80		7.2		
Er	0.65	9.6	85	2.46	6.7		6.7
Tm	0.67	7.6	92		4.6		
Yb	0.67	4.5	98		1.7		
Lu	-	0	-	-	0	0	-

Relevant parameters for the calculation of the paramagnetic correction factor β for rare earth 3+ ions. Column 6 shows the value of β-1 calculated from Eq. 10A. The corrected value of β-1 from Eq. 16A is given in column 7 for Pm and Sm. β-1 calculated from experimentally measured parameters using Eq. 12A is given in column 8 for comparison. All results are for a temperature of 300°K. Values in column 2 are from Ref. 54; column 3, Ref. 55, column 4, Ref. 56; column 5 Refs. 57 and 58.

REFERENCES

1. E. L. Brady and M. Deutsch, Phys. Rev. 78, (1950), 558.

2. H. Aeppli, H. Albers-Schönberg, A. S. Bishop, H. Frauenfelder and E. Heer, Phys. Rev. 84, (1951), 370.

3. H. Frauenfelder, Beta- and Gamma-Ray Spectroscopy, North-Holland Publ. Co., Amsterdam, (1955).

4. S. Devons and L. J. B. Goldfarb, Encyclopedia of Physics, Vol. 42, Springer-Verlag, Berlin (1957).

5. A. Abragam and R. V. Pound, Phys. Rev. 92, (1953), 943.

6. A. W. Schardt and J. P. Welker, Phys. Rev. 99, (1955), 810.

7. W. H. Kelly and M. L. Wiedenbeck, Phys. Rev. 102, (1956), 1130.

8. H. C. van den Bold, J. van de Geijn, and P. M. Endt, Physica 24, (1958), 23.

9. F. R. Metzger, Phys. Rev. 110, (1958), 123.

10. W. F. Edwards and C. J. Gallagher, Jr., Bull. Am. Phys. Soc. 4, (1959), 279; and private communication.

11. R. E. Holland, private communication

12. T. Lindquist and E. Karlsson, Ark. Fys. 12, (1957), 519.

13. E. Bodenstedt, E. Matthias, H. J. Körner and R. H. Siemssen, Z. Naturforshg. 13a, (1958), 425.

14. R. L. Graham and R. E. Bell, Can. J. of Phys., 31, (1953), 377.

15. V. Cappellar and R. Klingelhöfer, Z. Physik, 150, (1958), 375.

16. S. Koicki, J. Simic, and A. Kucoc, Nuclear Phys. 10, (1959), 412.

17. A. E. Blaugrund, Phys. Rev. Letters 3, (1959), 226.

18. S. G. Nilsson, Mat. Fys. Medd. Dan. Vid. Selsk. 29, (1955), no. 16.

19. E. D. Klema, Phys. Rev. 109, (1958), 1652.

20. Tor Wiedling, Thesis (University of Stockholm, 1956).

21. K. Alder, A. Bohr, T. Huus, B. Mottelson, and A. Winther, Revs. Mod. Phys. 28, (1956), 432.

22. M. Martin, P. Marmier, and J. de Boer, Helv. Phys. Acta 31, (1958), 435.

23. Tor Wiedling, Thesis (University of Stockholm, 1956).

24. S. Ofer, Nuclear Phys. 3, (1957), 479.

25. E. D. Klema, Phys. Rev. 109, (1958), 1652.

26. H. J. Behrend, Z. Naturforschg. 13a, (1958), 211.

27. S. E. Berlovich, Izvestia AN SSSR, ser. fiz. 20, (1956), 1438.

28. U. Hauser, private communication

29. G. Goldring and R. P. Scharenberg, Phys. Rev. 110, (1958), 701.

30. K. Sugimoto, Jour. of Phys. Soc. of Japan 13, (1958), 240.

31. B. Hartman and T. Wiedling, Ark. Fys. 10, (1956), 355.

32. S. Ofer, Nuclear Phys. 4, (1957), 477.

33. A. W. Sunyar, Phys. Rev. 98, (1955), 653.

34. J. Kanamori and K. Sugimoto, Jour. of Phys. Soc. of Japan, 13, (1958), 754.

35. G. D. Hickman and M. L. Wiedenbeck, Phys. Rev. 111, (1958), 539.

36. M. Deutsch, private communication

37. P. Debrunner, W. Kundig, J. Sunier and P. Scherrer, Helv. Phys. Acta 31, (1958), 326.

38. S. Ofer, Nuclear Phys. 5, (1958), 338.

39. R. G. Arns, R. E. Sund, and M. L. Wiedenbeck, Nuclear Phys. 11, (1959), 411.

40. F. K. McGowan, Phys. Rev. 85, (1955), 141.

41. J. S. Fraser and J. C. D. Milton, Phys. Rev. 98, (1955), 1173A.

42. J. Marklund, B. van Nooijen and Z. Grabowski, Nuclear Phys. 15, (1960), 555.

43. F. K. McGowan, P. R. 80, (1950), 923.

44. M. G. Mayer and J. H. D. Jensen, Elementary Theory of Nuclear Shell Structure, Chapman and Hall, London (1955).

45. A. Bohr and B. R. Mottleson, Mat. Fys. Med. Dan. Vid. Selsk. 27, (1953), no. 16.

46. B. R. Mottleson and S. G. Nilsson, Mat. Fys. Skr. Dan. Vid. Selsk. 1, (1959), no. 8.

47. G. Manning and J. D. Rogers, Nuclear Phys. 15, (1960), 166.

48. E. N. Hatch, F. Boehm, P. Marmier, and J. W. M. DuMond, Phys. Rev. 104, (1956), 745.

49. E. M. Bernstein and J. de Boer, to be published.

50. P. Marmier and F. Boehm, Phys. Rev. 97, (1955), 103.

51. A. Stendel, Naturwiss 44, (1957), 371.

52. E. N. Hatch, F. Boehm, P. Marmier, and J. W. M. DuMond, Phys. Rev. 104, (1956), 745.

53. D. R. Speck, Bull. Am. Phys. Soc. 1, (1956), 282.

54. R. J. Eliot and K. W. H. Stevens, Proc. Roy. Soc. A 218, (1953), 553; Proc. Roy. Soc. A 219, (1953), 387.

55. J. H. van Vleck, The Theory of Electric and Magnetic Susceptibilities, Clarendon Press, Oxford, (1932).

56. J. M. Balzer and B. Bleaney, Proc. Phys. Soc. A 68, (1955), 936.

57. K. D. Bowers and J. Owen, Reports on Prog. in Phys. 18, (1955), 304.

58. C. F. M. Cacho, M. A. Grace, C. E. Johnson, A. C. Knipper, and R. T. Taylor, Phil. Mag. 46, (1955), 1287.

59. K. Murawaka, Phys. Rev. 110, (1958), 393.

60. E. Bodenstedt, E. Matthais, H. J. Korner, E. Gerdau, H. Frisius, and D. Hovestadt, Nuclear Phys. 15, (1960) 239.